

PERFORMANCE EVALUATION OF NBI SUPPRESSION IN UWB-IR SYSTEM USING MMSE-RAKE RECEIVER

A DISSERTATION

*Submitted in partial fulfillment of the
requirements for the award of the degree
of*

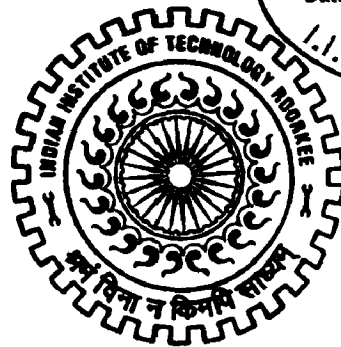
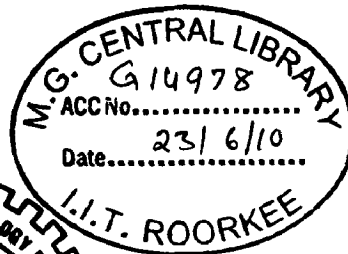
MASTER OF TECHNOLOGY

in

ELECTRONICS AND COMPUTER ENGINEERING
(With Specialization in Communication Systems)

By

LOVEKESH SINGH RAGHUWANSHI



DEPARTMENT OF ELECTRONICS AND COMPUTER ENGINEERING
INDIAN INSTITUTE OF TECHNOLOGY ROORKEE
ROORKEE-247 667 (INDIA)

JUNE, 2009

CANDIDATE'S DECLARATION

I hereby declare that the work, which is presented in this dissertation report entitled, **“PERFORMANCE EVALUATION OF NBI SUPPRESSION IN UWB-IR SYSTEM USING MMSE-RAKE RECEIVER”** towards the partial fulfillment of the requirements for the award of the degree of **Master of Technology** with specialization in **Communication Systems**, submitted in the Department of Electronics and Computer Engineering, Indian Institute of Technology Roorkee, Roorkee (India) is an authentic record of my own work carried out during the period from June 2008 to June 2009, under the guidance of **Dr. A. TYAGI, Assistant Professor, Department of Electronics and Computer Engineering, Indian Institute of Technology Roorkee.**

I have not submitted the matter embodied in this dissertation for the award of any other Degree or Diploma.

Date: 30/06/09

Place: Roorkee

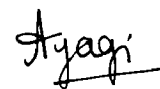

LOVEKESH SINGH RAGHUWANSHI

CERTIFICATE

This is to certify that the above statement made by the candidate is correct to the best of my knowledge and belief.

Date: 30/06/09

Place: Roorkee


Dr. A. TYAGI,
Assistant Professor, E&C Department,
IIT Roorkee,
Roorkee – 247 667 (India).

ACKNOWLEDGEMENTS

It is my privilege and pleasure to express my profound sense of respect, gratitude and indebtedness to my guide, Dr. Anshul Tyagi, Assistant Professor, Department of Electronics and Computer Engineering , Indian Institute of Technology, Roorkee, for his inspiration, guidance, constructive criticisms and encouragement throughout this dissertation work.

Thanks are due to the Lab staff Communication systems Lab, Department of electronics and Computer Engineering, IIT Roorkee for providing necessary facilities.

I gratefully acknowledge my sincere thanks to my family members for their inspirational impetus and moral support during course of this work.

The pleasure of nearing completion of the course requirements is immense, but with it carries the pain of leaving behind these wonderful two years of life in the sprawling green campus of this great historical institute. I proud myself to being the student of this reputed institute.

I am greatly indebted to all my friends, who have graciously applied themselves to the task of helping me with ample morale support and valuable suggestions. Finally, I would like to extend my gratitude to all those persons who directly or indirectly helped me in the process and contributed towards this work.

LOVEKESH SINGH RAGHUWANSHI

ABSTRACT

Ultra Wideband Technology for commercial communication application is a recent innovation. Short-range wireless systems have recently gained a lot of attention to provide multimedia communications and to run high speed applications around a user centric concept in so called Wireless Personal Area Networks (WPAN). UWB technology presents itself as a good candidate for the physical layer of the WPAN.

In February 2002, the FCC issued a ruling that ultra-wideband (UWB) could be used for data communications as well as for radar and safety applications. UWB system is constrained to have a maximum power transmission of -41 dBm and a bandwidth ranging from 3.1-10.6 GHz. UWB co-exists and does not interfere with the existing narrowband or wideband communication systems in the same spectrum. However, due to its low power in the same bandwidth, UWB is affected by the so-called narrowband interference (NBI). This report presents a method to eliminate the narrowband interference in UWB system.

The TH-UWB system performance was analyzed in a realistic UWB frequency selective channel and in the presence of NBI for RAKE receiver. We demonstrated that TH reduces the impact of multiuser interference but does not combat NBI. To suppress NBI, a Partial Rake receiver used. It consists of selecting the first strongest multipath components using an appropriate Rake receiver with the path diversity combining being based on the minimum mean square error criterion.

The design correctness has been validated by means of simulation using standard UWB IEEE standard channel models, Time Hopping-Pulse Position Modulation and the rake receiver technique with the path diversity combining being based on the minimum mean square error criterion.

CONTENTS

CANDIDATE'S DECLARATION	i
ACKNOWLEDGEMENTS	ii
ABSTRACT	iii
CONTENTS	iv
LIST OF FIGURE	vii
TABLE OF ABBREVIATIONS	ix
CHAPTER 1: Introduction	1
1.1 Ultra Wideband Overview	1
1.2 Modulation	2
1.3 Fractional Bandwidth	3
1.4 Narrowband Overview	6
1.5 Literature Review	8
1.6 Organization of Report	9
CHAPTER 2: UWB Transmission	11
2.1 Monocycle Waveform	11
2.2 UWB Channel	15
2.2.1 Slow Fading	15
2.2.2 Fast Fading	16
2.2.3 Flat Fading	17
2.2.4 Frequency Selective Fading	17
2.3 Multipath Propagation	18
2.3.1 Reflection	19
2.3.2 Diffraction	19
2.3.2 Scattering	19
2.4 Channel Modeling	19
2.5 Multiple Access Schemes	21

CHAPTER 3: Rake Receiver	22
3.1 Introduction	22
3.2 Diversity and RAKE Receiver	23
3.3 Common Diversity Techniques	24
3.3.1 Selection Diversity	25
3.3.2 Maximal Ratio Combining	25
3.3.3 Equal Gain Combining	25
3.3.4 Minimum Mean Square Error Combining	26
3.4 Working of RAKE Receiver	26
CHAPTER 4: The UWB Radio and WLAN Based OFDM Signal	31
4.1 UWB Transmitter Structure	31
4.2 UWB Receiver Structure	32
4.3 Generation of TH-PPM-UWB Signal	32
4.4 IEEE 802.11a OFDM WLAN Transmitter Structure	35
4.5 IEEE 802.11a OFDM WLAN Receiver Structure	36
4.6 Generation of IEEE 802.11a OFDM WLAN Signal	36
CHAPTER 5: NBI Suppression	38
5.1 Introduction	38
5.2 TH-PPM-UWB System Model	39
5.3 MMSE-RAKE Receiver for UWB System	41
5.4 Calculation of the MMSE-RAKE Optimal Weight	46
5.5 System Average Bit Error Rate	46
CHAPTER 6: Simulation Results and Discussion	49
6.1 Simulation Set-up	49
6.2 Simulation Parameters	50
6.3 Simulation Results	51
6.3.1 BER of Different Number of MMSE-RAKE Finger	52

6.3.2	BER for MMSE-RAKE Receiver for Different TH-Sequence	54
6.3.3	BER for MMSE-RAKE Receiver for Different SIR	57
	CONCLUSION AND FUTURE WORK	59
	REFERENCES	60

List of Figures

- 1.1 Modulation Techniques
- 1.2 Energy Bandwidth
- 1.3 FCC UWB Spectral Masks
- 2.1 Gaussian Derivative Waveform
- 2.2 Monocycle Waveforms
- 2.3 Higher Order Derivative of Gaussian pulse waveforms
- 2.4 Typical slow and fast fading
- 2.5 TH and DS-UWB-IR Signaling Structure
- 3.1 Rake Receiver with N_R Parallel Correlators
- 3.2 Rake Receiver with N_R Parallel Correlators and Time Delay Unit
- 3.3 RAKE Receiver for Discrete-Time Channel Models
- 4.1 A General UWB Transmitter Block Diagram
- 4.2 A General UWB Receiver Block Diagram
- 4.3 Transmission Scheme for TH-PPM-UWB System
- 4.4 TH-PPM-UWB Signal
- 4.5 Block Diagram of a Typical OFDM Transmitter (IEEE 802.11a Standard)
- 5.1 MMSE-Rake Receiver Model for TH-PPM-UWB System
- 6.1 Simulation Block Diagram
- 6.2 BER Performance for Partial MMSE-RAKE Receiver
- 6.3 BER Performance for Selective MMSE-RAKE Receiver
- 6.4 BER Performance for Different MMSE-RAKE Receiver
- 6.5 BER Performance for All MMSE-RAKE Receiver for Different Time Hopping Sequence ($N_h = 5$ and $N_h = 10$)
- 6.6 BER Performance for Selective MMSE-RAKE Receiver for Different Time Hopping Sequence (for $F_n = 8$, $N_h = 5$ and 10)
- 6.7 BER performance for Partial MMSE-RAKE receiver for Different Time Hopping Sequence (for $F_n = 8$, $N_h = 5$ and 10)

- 6.8 BER performance for All MMSE-RAKE receiver for different SIR
(SIR = -10dB and -20dB)
- 6.9 BER performance for Selective MMSE-RAKE receiver for different SIR
(SIR = -10dB and -20dB)
- 6.10 BER performance for Partial MMSE-RAKE receiver for different SIR
(SIR = -10dB and -20dB)

Table of Abbreviations

A-RAKE	All RAKE
AWGN	Additive White Gaussian Noise
BPSK	Binary Phase Shift Keying
BER	Bit Error Rate
CDMA	Code Division Multiple Access
CP	Cyclic Prefix
DS	Direct Sequence
EGC	Equal Gain Combining
FCC	Federal Communications Commission
IEEE	Institute for Electrical and Electronics Engineers
IR	Impulse Radio
MAI	Multiple Access Interference
MHz	Mega Hertz
MMSE	Minimum Mean Square Error
MRC	Maximum Ratio Combining
NBI	Narrowband Interference
OFDM	Orthogonal Frequency Division Multiplexing
PPM	Pulse Position Modulation
P-RAKE	Partial RAKE
PSD	Power Spectral Densities
SD	Selection Diversity
SIR	Signal to Interference Ratio
SNR	Signal to Noise Ratio
S-RAKE	Selective RAKE
TH	Time Hopping
UWB	Ultra Wideband
WLAN	Wireless Local Area Network

Chapter 1

Introduction

The most influential milestone in the history of Ultra Wideband (UWB) wireless communications was set in April 2002 when the Federal Communications Commission (FCC) approved the first guidelines allowing UWB signals contained within specified emission masks [1]. Ultra-Wideband (UWB) systems spread the transmitted signal power over an extremely large frequency band, and the power spectral density of the signal is very low. Due to the wide bandwidth of the transmitted signal, UWB signal energy will spread over the frequency bands allocated to other existing radio systems. Coexisting with many concurrent narrowband services, the performance of UWB systems will be affected considerably by them due to the high power of these narrow-band signals with respect to the UWB signals. Specifically, IEEE 802.11a systems which operate around 5 GHz and overlap the band of UWB signals will interfere with UWB systems significantly. Evaluating interference issues of these narrowband systems to UWB systems in its overlay band is an important issue for us to understand and design efficient UWB systems. This report describes what UWB is, and the importance of this technology in its coexistence with other technologies in the same spectrum (NBI). Sharing spectrum causes problems in UWB communications, which motivate for this work.

1.1 Ultra Wideband Overview

Historically, UWB radio systems were mainly developed as a military tool because they have acquired high capability to scan through trees and beneath ground surfaces. Recently, UWB technology has been focused on consumer electronics and communications. Although UWB systems are years away from being ubiquitous, UWB technology is changing wireless industry today. UWB technology is different from the conventional narrowband wireless transmission technology. Instead of broadcasting on separate frequencies, UWB spreads signals across a very wide frequency range. The signals are transmitted in sequences of very short pulses rather than continuous waveforms using Radio Frequencies (RF) carrier as in narrowband (NB) communication systems. This technique has been extensively used in radar applications and went under the name of Impulse Radio (IR).

The most remarkable roadmap in UWB wireless communications was regulated in April 2002 by FCC. However, according to the FCC rules, UWB concept is not limited to the pulsed transmission but can be extended to continuous-like transmission techniques, providing the occupied bandwidth of the transmitted signal is greater than 500 MHz. The general consensus establishes that a signal is UWB if its bandwidth is large with respect to the carrier or center frequency of the spectrum. In other words, the fractional bandwidth is as high as 0.2-0.25 percent of its central frequency. These pulses or waveforms, because of their large bandwidth, must, at least in principle, co-exist in a friendly manner with other Hertzian waveforms present in the air interface. The coexistence principle introduces strict limitations over Power Spectral Densities (PSD) and raises the issue of designing power efficient networks in addition to the narrowband interference (NBI) avoidance in UWB communication systems. The following section describes the modulation techniques that are most commonly used in the UWB systems.

1.2 Modulation

Modulation methods for UWB systems can be categorized in two types: time-based techniques and shape-based techniques. For pulsed UWB systems, the most commonly used modulation techniques include Pulse Position Modulation (PPM), Pulse Amplitude Modulation (PAM) and On-Off Keying (OOK). PPM is a time-based technique; PAM and OOK belong to the shape-based techniques. Figure 1.1 [2] describes the most popular modulation techniques considered for UWB system

- **On-Off Keying:** On-Off Keying (OOK) signaling is one of the earliest modulation types; bit value 1 is represented by the presence of a pulse, and the absence of a pulse for bit 0.
- **Pulse Position Modulation:** Pulse Position Modulation (PPM) is the most popular method of modulation in the literature. In a PPM-UWB system, bit value 1 is represented by a pulse with delay relative to the time reference and bit 0 is represented by a pulse without any delay.
- **Pulse Amplitude Modulation:** For binary pulse amplitude modulation, the information bit is transmitted by modulating the pulse polarity.

- **Combined Modulation:** Combined modulation schemes such as PAM / M-PPM and PAM/OOK could improve capacity or throughput at the cost of complexity

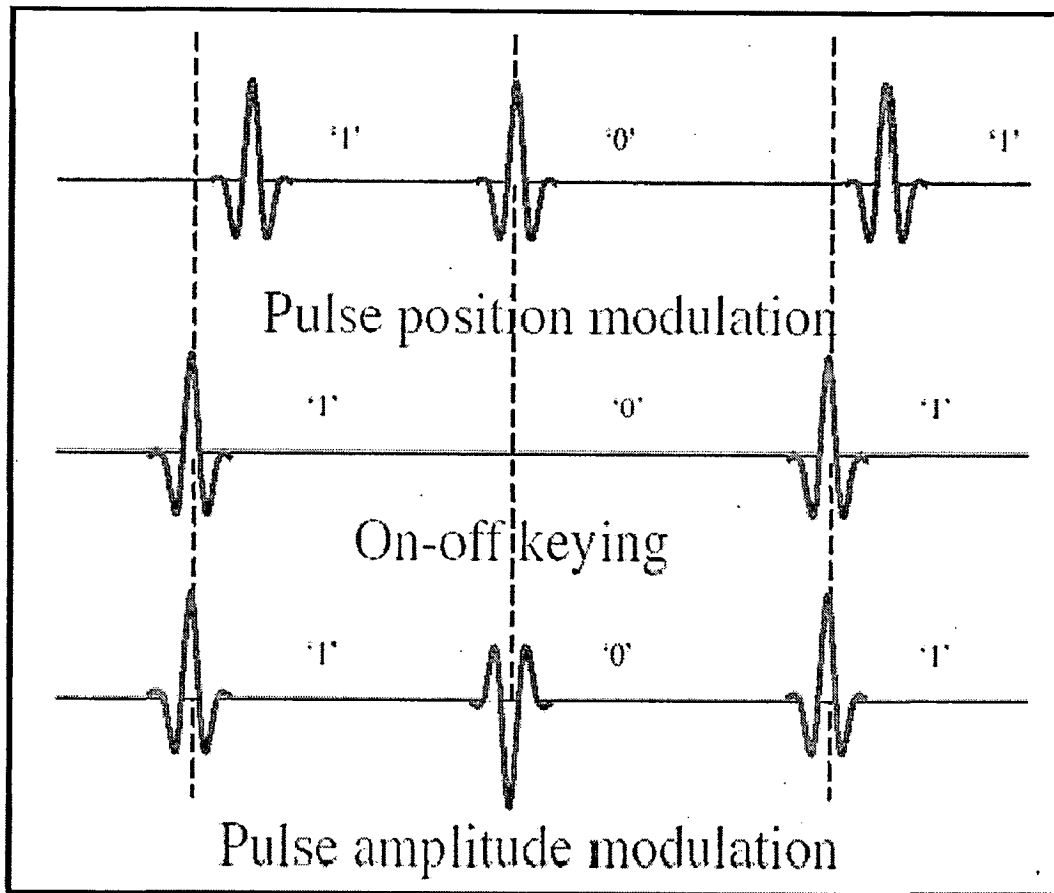


Figure 1.1 Modulation Techniques.

1.3 Fractional Bandwidth

As mentioned earlier, the term UWB comes from the radar world and refers to electromagnetic waveforms that are characterized by an instantaneous fractional energy bandwidth greater than 0.2-0.25. Let E be the instantaneous energy of the waveform, the energy bandwidth is then identified by the frequencies f_L and f_H , which delimited the interval where most of the energy E (i.e., over 90%) is captured. The width of the interval $[f_L, f_H]$ is called energy bandwidth as shown in Figure 1.2 [1]. Note that if f_L is the lower limit and f_H is the upper limit of the Energy Spectral Density (ESD) and the center frequency of the spectrum is located at $(f_L + f_H)/2$.

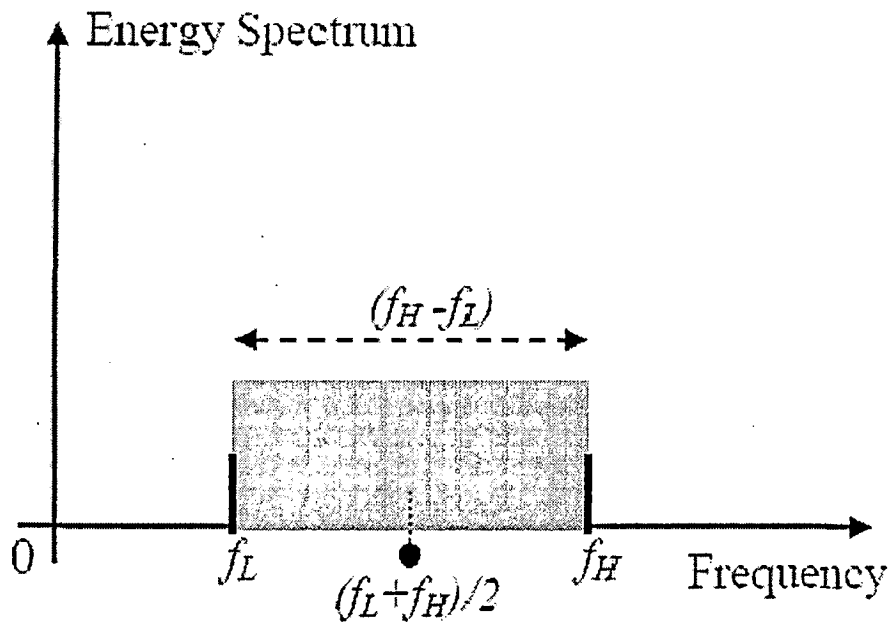


Figure 1.2 Energy Bandwidth.

Fractional bandwidth is defined as the ratio of the energy bandwidth and the center frequency and expressed as:

$$\text{Fractional bandwidth} = \frac{(f_H - f_L)}{\left\{ \frac{(f_H + f_L)}{2} \right\}}$$

According to the FCC's first report and order in April 2002, UWB systems with $f_c > 2.5$ GHz need to have a -10dB bandwidth of at least 500 MHz, while UWB systems with $f_c < 2.5$ GHz need to have fractional bandwidth at least 0.20. A signal with an energy bandwidth of 2 MHz, for example, is UWB if the center frequency of its spectrum is lower than 10 MHz.

Often the term “percent bandwidth” is used for UWB system. Percent bandwidth is simply the fractional bandwidth in percentage units. Also its use in the relative bandwidth which is equal to half of the fractional bandwidth. Relative bandwidth represents the ratio between half of the energy bandwidth and the center frequency.

There are different ways to choose the lower and upper limit frequencies depending on how stringent the requirement on the bandwidth is set. For example, in a recent release of UWB emission masks in the United States (FCC, 2002), the f_L and f_H are set to be the lower and upper frequencies of the -10dB emission points. The selection of -10 dB over the -20 dB bandwidth established by the Defense Advance Research Projects Agency (DARPA) [3] is motivated by the fact that UWB emission is permitted at lower power levels, which are close to the noise floor.

Under these conditions, the -20 dB emission points cannot be measured correctly. Within the FCC, 2002 regulation, a signal is always assumed to be UWB if its bandwidth at -10dB emission point exceeds 500 MHz, regardless of the fractional bandwidth values.

To summarize, some of UWB's potential advantages

- (i) Low power operation since transceiver circuitry power requirements are low
- (ii) UWB transmissions are below the noise level thereby providing low probability of detection (LPD)
- (iii) Low probability of jamming (LPJ) capabilities due to the low energy per frequency band and the use of precisely timed patterns
- (iv) Ability to penetrate walls and vegetation due to the lower frequencies used
- (v) Higher immunity to multipath fading effects due to increased diversity
- (vi) Availability of precise location information, since UWB uses precise pico-second pulses for transmission and tight synchronization between the communicating nodes, which enables centimeter-accurate location determination.

However, UWB has a few disadvantages such as long signal acquisition times (up to a few milliseconds), and FCC regulatory issues. There are also several technical challenges at the physical layer to be resolved such as: antenna design, propagation and channel modeling, devices and circuits design, and waveform design.

Applications

UWB has several applications all the way from wireless communications to radar imaging, and vehicular radar. The ultra wide bandwidth and hence the wide variety of material penetration capabilities allows UWB to be used for radar imaging systems, including ground penetration radars, wall radar imaging, through-wall radar imaging, surveillance systems, and medical imaging. Similarly, the excellent time resolution and accurate ranging capability of UWB can be used for vehicular radar systems for collision avoidance, guided parking, etc. Last but not least is the wireless communication application, which is arguably the reason why UWB became part of the wireless world, including wireless home networking, high-speed WPAN/WBAN, wireless sensors networks, wireless telemetry, telemedicine, etc.

1.4 Narrowband Overview

Narrowband (NB) refers to a signal which occupies only a small amount of spaces on the radio spectrum. Narrowband is opposite to the broadband or wideband (WB). In the study of wireless communications such as a UWB system, narrowband implies that the bandwidth under consideration is sufficiently “narrow” compared to the UWB bandwidth [4]. The Narrowband in study for indoor communications is the wireless local access network (WLAN) based Orthogonal Frequency Division Multiplexing (OFDM) signal.

This WLAN system is also known as the third wireless generation and has been used to offer maximum data rate at a central frequency in the 5 GHz frequency band. The standardization of this wireless generation is taking place simultaneously in the U.S., Japan and Europe. The Institute for Electrical and Electronics Engineers (IEEE) is working on WLAN and models is known as IEEE 802.11a standard. The standard is based on the OFDM modulation scheme having a bandwidth of 16 MHz per subcarrier in OFDM. The modulation scheme ranges from BPSK up to 64-QAM. Together with a variable error-coding rate, OFDM modulation allows the data rate to be adapted from 6 Mbit/s to 54 Mbit/s, depending on the propagation channel conditions. The IEEE 802.11a is the primary interference for indoor UWB communication systems. Interference concept is to be discussed in the subsequent section.

Interference

A Wideband system, by its nature, interferers with the existing Narrowband services in the same frequency band and in turn, the Narrowband signals act as interferers to the Wideband system. The extent to which performance is degraded by the interference clearly depends on the number and distribution of the interferers, the relative power between Wideband and Narrowband signal and the type of modulation of the two signals. With respect to transmission power, FCC specifications and European standards [4], essentially limit the equivalent isotropically radiated power (EIRP) to US Part 15 limits, that is, -41 dBm/MHz for UWB in the range of frequency from 3.1-10.6 GHz. To be UWB, the signal must occupy an instantaneous bandwidth of at least 500 MHz. Figure 1.3 [5] in next page illustrates the FCC UWB spectral masks.

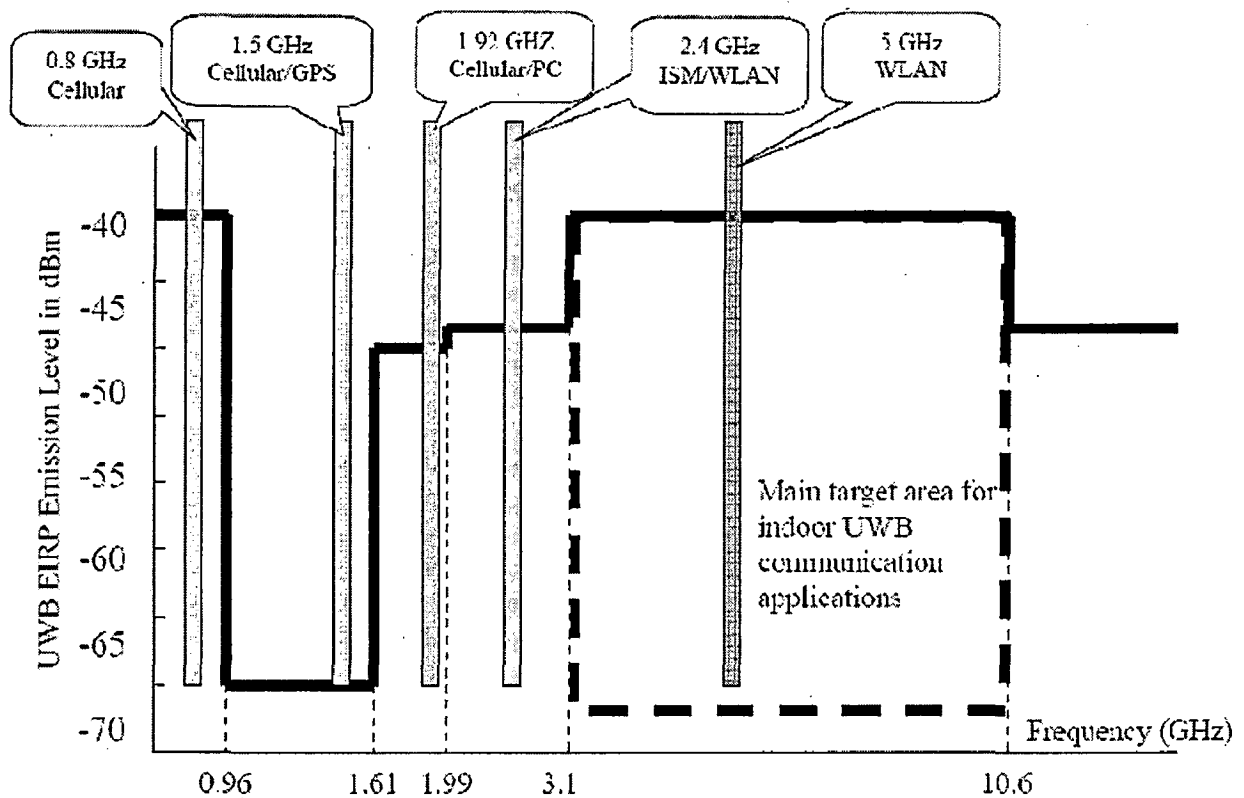


Figure 1.3 FCC UWB Spectral Masks.

As mentioned earlier, the primary narrowband interference occupies within the indoor UWB communication system is the IEEE802.11a, in particular the OFDM based WLAN signal, the power spectrum density for NBI scenario is shown in Figure 1.3. In contrast to the UWB, the WLAN NB allowed emission is +40 dB/MHz, which may be expected to be 10-12 dB above the noise floor while the UWB emission below this noise level. As the result, the presence of Narrowband may cause severe degradation in the performance of UWB systems.

Figure 1.3 shows within the spectrum of interested, the narrowband interference (NBI) is the 5 GHz OFDM based WLAN signal. There are works studying degradation in the performance of UWB radios due to narrowband interference within the 3.1-10.6 GHz frequency range, such as tone jammers [5], partial band interference (PBI) [6] and WLAN IEEE 802.11a interference [7].

1.5 Literature Review

Ultra wide bandwidth (UWB) systems must share their large bandwidth with coexisting narrowband applications. Although UWB signals may enjoy inherently high spreading gain, stringent Federal Communications Commission power restrictions make them susceptible to strong narrowband interference (NBI), which can severely degrade performance. The extent of performance degradation depends on the number, power, and spatial distribution of the interferers relative to the UWB signal. NBI may be tens of decibels stronger than the UWB signal [8] and can completely overwhelm the receiver front end. Severe NBI could thus render the acquisition process impossible, and front-end interference mitigation techniques are desirable. Some NBI mitigation techniques have been proposed for UWB. However, most of these techniques are based on traditional spread-spectrum methods, which might not be suitable for UWB applications. The design of NBI mitigation algorithms tailored for UWB systems is thus still largely an open research issue.

Several research efforts have investigated the impact of NBI on UWB. An analysis of the effect of single tone interferers on TH-UWB systems is presented in [9], while the effect of tone interferers on UWB system in multipath fading scenarios is analyzed in [10]. In [11], the effect of NBI on direct-sequence based impulse radio (DS-UWB) is derived, where NBI is modeled as the sum of sinusoidal signals with variable power and frequency. The performance of a generalized Rake receiver in the presence of multiple access interference and NBI is analyzed in [12]. The impact of NBI on DS-UWB as well as single and multicarrier multiband UWB is discussed in [13] and [14]. The effect of the Global System for Mobile Communications and the Universal Mobile Telecommunications System/Wideband Code-Division Multiple-Access bands on UWB is studied in [15], where it is shown by simulation that performance degradation is most severe when the NBI bandwidth overlaps with the UWB nominal center frequency.

Some NBI mitigation techniques for UWB systems have been proposed in the literature. Various pulse-shaping methods that introduce nulls in the UWB spectrum where NBI occurs are investigated in [16]–[19]. However, these methods assume knowledge of the NBI spectrum. The performance of a direct-sequence coded division multiple access (DS-CDMA) UWB systems in the presence of NBI has been considered in [12] using a maximal ratio combining (MRC) technique. This combining technique can alleviate the effect of multiple-access interference (MAI) on the system performance, but does not suppress NBI. In [20], the performance of a

multiuser receiver for a DS-CDMA UWB system in the presence of an IEEE 802.11a OFDM signal modeled as a Gaussian noise was investigated based on a Gaussian approximation for the multiuser interference. Under this particular assumption, the system was shown to be able to support a very large number of users for a given single user bit error rate (BER). Hence, it is very important to assess the accurate TH-UWB system performance. To the best of our knowledge, all previous multi-access TH-UWB system investigations in a frequency selective channel considered the Gaussian approximation assumption for the multiuser interference. In order to accurately evaluate the UWB system performance, a study without the use of this assumption and in a realistic UWB propagation environment is required.

1.6 Organization of Report

Chapter 2 discussed about Monocycle waveform that is used as pulse shape for transmitting UWB signal. Monocycle waveform is nanosecond pulse that is generate from 1st or 2nd order derivative (or can be higher order derivative) of Gaussian waveform. Fading and multipath phenomenon also discussed as UWB signal propagate through it. Apart from that Saleh-Valenzuela and IEEE 802.15.3a based Mathematical model of UWB channel is described.

Chapter 3 discussed mathematical analysis of RAKE receiver that is used in this report for NBI suppression and also described various type of RAKE receiver such as A-RAKE, S-RAKE and P-RAKE. Apart from that different diversity techniques that is used in RAKE receiver such as SD, MRC, EGC and MMSE is described. From that MMSE diversity technique used in this report.

Chapter 4 discussed mathematical analysis and methods to generate a UWB signal as well as OFDM based WLAN signals. Impulse radio methods based generation of pulses that are very short in time and TH-PPM are described. The methods of generating non-impulsive signal such as OFDM are also covered.

Chapter 5 discussed mathematical model of TH-PPM-UWB system and also described mathematical analysis of MMSE-RAKE receiver for NBI suppression in TH-PPM-UWB system.

Apart from that Using MMSE, find optimal weight for combine RAKE receiver output and suppress NBI.

Chapter 6 discussed simulation result for NBI suppression based on mathematical analysis from chapter 2 to chapter 5. Simulation result shows that NBI suppression can be achieved in TH-PPM-UWB system using MMSE-RAKE receiver. IEEE 802.15.3a based CM1 (LOS 0-4 m) UWB channel is considered for UWB transmission. And also compare the BER performance of A-RAKE, S-RAKE and P-RAKE receiver for different TH sequence and different SIR.

Chapter 2

UWB Transmission

UWB usually refers to impulse based waveforms that can be used with different modulation schemes. The transmitted signal consists of a train of very narrow pulses at base band, normally of the order of a nano second. Each transmitted pulse is referred to as a monocycle. The information can be carried by the position or amplitude of the pulses.

2.1 Monocycle Waveforms

The frequency-domain spectral content of a UWB signal depends on the pulse waveform shape and the pulse width. Typical pulse waveforms used in research include [4], [21]

- Rectangular
- Gaussian
- Gaussian doublet, and
- Rayleigh monocycles, etc.

A monocycle should not have zero DC component to allow it to radiate effectively. A rectangular monocycle with width T_p can be represented by $[u(t) - u(t - T_p)]$, where $u(\cdot)$ denotes the unit step function. The rectangular pulse has a large DC component, and the antennas do not radiate at direct current (dc), which is not a desired property.

In most of the cases for communication purpose Gaussian pulses and its derivatives are used. The reason behind the popularity of these pulses is twofold:

- i) Gaussian pulses come with the smallest possible time-bandwidth product of 0.5, which maximizes range-rate resolution
- ii) The Gaussian pulses are readily available from the antenna pattern [1]. A generic Gaussian pulse is given by

$$P_g(t) = \frac{1}{\sqrt{2\pi}\sigma} e^{-\frac{1}{2}\left(\frac{t-\mu}{\sigma}\right)^2} \quad (2.1)$$

Where μ defines the center of the pulse and σ determines the width of the pulse. Even the basic Gaussian pulse contains a dc term, and therefore, it cannot be used as a UWB pulse.

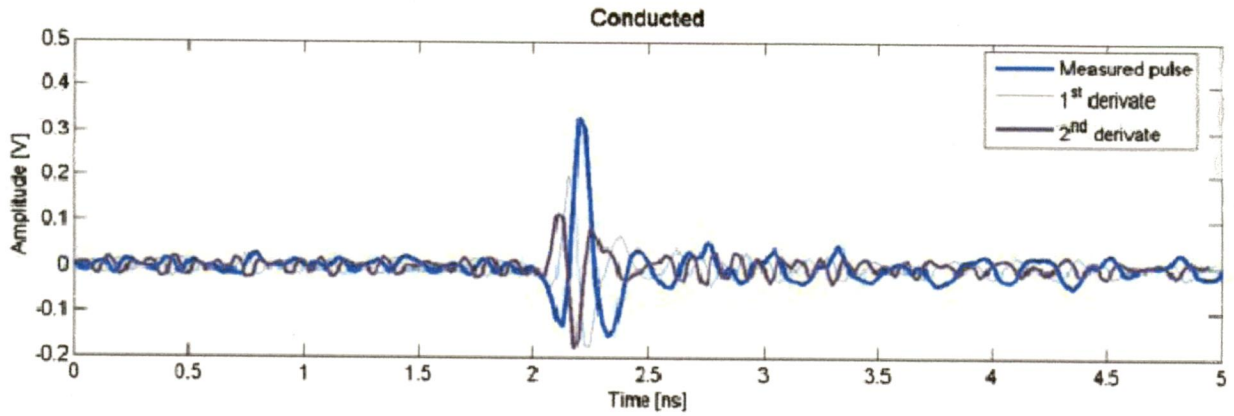


Figure 2.1 Gaussian Derivative Waveform.

Some monocycles are derived from the Gaussian pulse as shows in fig 2.1 [4]. The Gaussian monocycle is the second derivative of a Gaussian pulse, and is given by

$$P_g(t) = A_G \left[1 - \left(\frac{t - \mu}{\sigma} \right)^2 \right] e^{-\frac{1}{2} \left(\frac{t - \mu}{\sigma} \right)^2} \quad (2.2)$$

Where the parameter σ determines the monocycle width T_p . The effective time duration of the waveform that contains 99.99% of the total monocycle energy is $T_p = 7\sigma_p$ centered at $\mu = 3.5\sigma$. The factor A_G introduced so that the total energy of the monocycle is normalized to unity.

The Rayleigh monocycle is derived from the first derivative of the Gaussian pulse as shown in fig 2.2 and is given by

$$P_R(t) = A_R \left[\frac{t - \mu}{\sigma^2} \right] e^{-\frac{1}{2} \left(\frac{t - \mu}{\sigma} \right)^2} \quad (2.3)$$

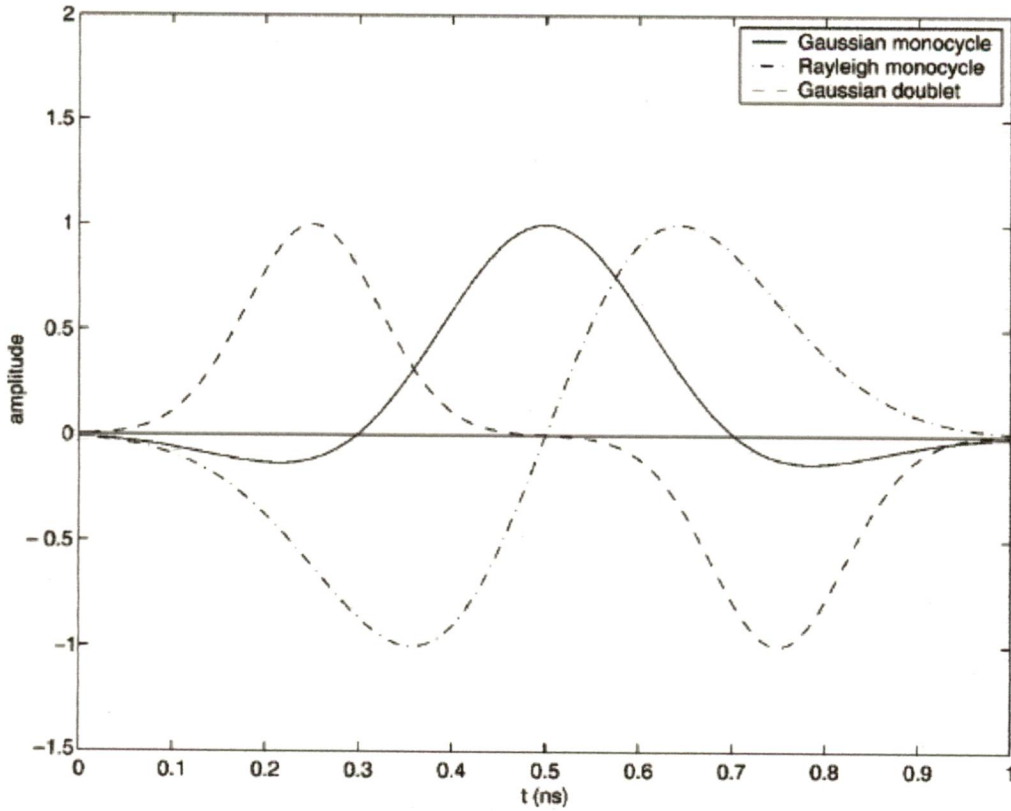


Figure 2.2 Monocycle Waveform.

Even The recursive presentation for the higher order (n-th order) derivatives of the Gaussian pulse depicted in Fig 2.3. can be derived by [4]

$$W^{(n)}(t) = -\frac{n-1}{\sigma^2} W^{(n-2)}(t) - \frac{t}{\sigma^2} W^{(n-1)}(t) \quad (2.4)$$

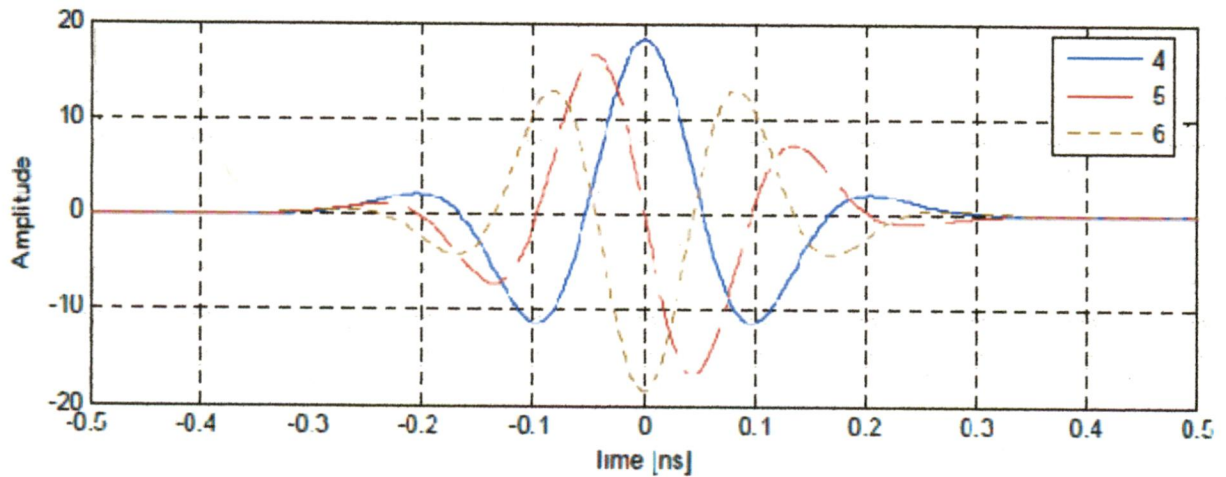


Figure 2.3 Higher order Derivative of Gaussian pulse waveforms.

The amplitude spectrum of the Gaussian pulse, $W(f)$, thus the presentation of $W(f)$ in the frequency domain, can be derived from [1] and given by

$$|W_n(f)| = A(2\pi f)^n \exp\left\{-\frac{(2\pi f\sigma)^2}{2}\right\} \quad (2.5)$$

The power spectral density for the n-th order Gaussian pulse is then derived by [2]

$$|P_n(f)| = A_{max} \frac{(2\pi f\sigma)^{2n} \exp\{-(2\pi f\sigma)^2\}}{n^n \exp(-n)} \quad (2.6)$$

where A_{max} scales the normalized power spectral density under the radiation regulations and f is frequency. Table 2.1 shows the center frequency and -10 db bandwidth used in Gaussian pulse and derivative of Gaussian pulse.

TABLE 2.1
Center Frequencies and -10dB Bandwidth for the used Pulse waveform

Generated Pulse waveform	f_c	B_{-10dB}
Gaussian Pulse	$1/T_P$	$2/T_P$
Gaussian Doublet	$1/T_P$	$2/T_P$
2 nd derivative of Gaussian Pulse	$1.73/T_P$	$2.1/T_P$
3 rd derivative of Gaussian Pulse	$2/T_P$	$2/T_P$

Criteria

Important criteria in designing the monocycle waveform include:

1. Simplicity of the monocycle generator, and
2. Minimal interference between the UWB system and other narrowband system coexisting in the same frequency band

2.2 UWB Channel

While a UWB signal propagates in a channel, it follows the phenomenon of fading and multipath. In this section we will discuss about fading and multipath and then discuss about the UWB channel model.

Fading

Fading is one of the most challenging problems faced in a mobile or wireless signal propagation system. Fading is the time variation of the received signal power caused by the changes in the transmission medium or paths. In case of the fixed environments, fading is affected by changes in the atmospheric conditions, for example by the presence of moisture in atmosphere, rainfall etc [22].

Fading effects can be classified as either slow or fast. They can also be classified in terms of flat and frequency selective fading. Figure 2.4 depicts the typical slow and fast fading behaviors [22].

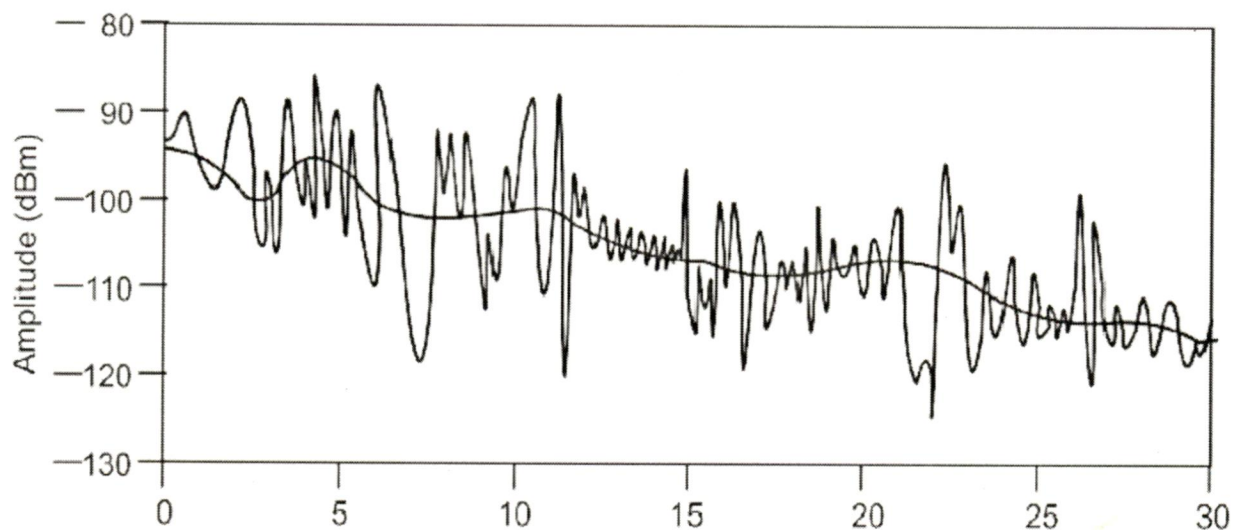


Figure 2.4 Typical slow and fast fading.

2.2.1 Slow Fading

If the channel impulse response changes at a rate much slower than the transmitted baseband signal, let say $s(t)$, then it's a slow fading channel. The channel may be static over one or several reciprocal bandwidth intervals [23]. If we talk in terms of the frequency domain, then

we can say that the Doppler spread of the channel is much less than the bandwidth of the baseband signals [23]. Hence we observe a slow fading if

$$T_S \ll T_C$$

And

$$B_S \gg B_D$$

B_D is Doppler spread and it is a measure of the spectral broadening caused by the time rate of change of the mobile radio channel and is defined as the range of frequencies over which the received Doppler spectrum is essentially non-zero. If we wish to define Doppler spectrum then it's the case when after we have transmitted a pure sinusoidal tone of frequency f_c , the received signal spectrum will have the components in the range of $f_c - f_d$ and $f_c + f_d$, where f_d is the Doppler shift.

B_S is the band width of the transmitted signal or modulation. T_S is the reciprocal of bandwidth e.g. symbol period. T_C is coherence time and it is the time domain dual of the Doppler spread and is used to characterize the time varying nature of the frequency dispersive ness of the channel in the time domain. It is interesting to note that Doppler spread and coherence time are inversely proportional to one another i.e.

$$T_C = 1/f_m$$

2.2.2 Fast Fading

If the channel impulse response changes rapidly within the symbol duration, the channel is known as fast fading channel. It implies that the coherence time of the channel is smaller than the symbol period of the transmitted signal. Due to this, frequency dispersion happens. Doppler spreading contributes in it too. Frequency dispersion is also called as time selective fading and it will be discussed later on in this chapter. If we look in the frequency domain, signal distortion due to fast fading increases with increasing Doppler spread relative to the bandwidth of the transmitted signal. Hence, signal undergoes fast fading if [23]

$$T_S > T_C$$

And

$$B_S < B_D$$

We still have to discuss about the flat fading and selective fading. In context of these two fading, it should be noted that when we talk about the fast or slow fading we do not specify that if the channel is flat or selective faded. Fast fading only concerns with the rate of change of channel due to motion. Here we also ascertain that velocity of the mobile or in other words velocity of the objects in the channel and baseband signaling dictates that if the channel undergoes fast or slow fading.

2.2.3 Flat Fading

A received signal will undergo flat fading if the mobile radio channel has a linear phase response over a bandwidth which is greater than the bandwidth of the transmitted signal and constant gain. This is the most common type of fading and traditionally discussed in the technical literature. One of the characteristics of flat fading is the perseverance of the spectral characteristics of the transmitted signal at the receiver. The strength of the received signal changes with time and it is due to multipath which is causing fluctuations in the gain of the channel. To summarize the flat fading let us have the following equations

$$T_S \gg \sigma_\tau$$

And

$$B_S \ll B_C$$

where B_S is the bandwidth of the transmitted signal or modulation. T_S is the reciprocal bandwidth e.g. symbol period. B_C is the coherence bandwidth and it is defined as the statistical measure of the range of frequencies over which the channel can be considered “flat” i.e. a channel which passes all spectral components with equal gain and linear phase [23]. σ_τ is the rms delay spread and it is defined as the square root of the second central moment of the power delay profile.

2.2.4 Frequency Selective Fading

The channel creates frequency selective fading if it possesses a constant gain and linear response over a bandwidth that is smaller than the bandwidth of the transmitted signal. The received signal includes multiple versions of the transmitted waveform which are attenuated, faded, and delayed in time. This results in a distorted signal. The channel induces intersymbol interference. If we look in the frequency domain, certain frequency components in the received signal spectrum have greater gain than in others [23].

Frequency selective fading channels are also known as wideband channels since the bandwidth of the signal is wider than the bandwidth of the channel impulse response. We can depict the behavior of a frequency selective fading channel by the following equations.

$$T_S < \sigma_\tau$$

And

$$B_S > B_C$$

where T_S is the reciprocal bandwidth, B_S is the bandwidth of the transmitted modulation, σ_τ and B_C are the rms delay spread and coherence bandwidth.

2.3 Multipath Propagation

In the previous section we have discussed about fading. Let us consider the principle factor which is the cause of this phenomenon. Fading is caused by interference between two or more versions of the transmitted signal which arrive at the receiver at slightly different times. These waves, called multipath waves, combine at the receiver antenna to give a resultant signal which can vary widely in amplitude and phase, depending on the distribution of the intensity and relative propagation time of the waves and the bandwidth of the transmitted signal [23].

Multipath in the radio channel creates small-scale fading effects. The three most important effects are:

1. Rapid changes in signal strength over a small travel distance or time interval
2. Random frequency modulation due to varying Doppler shifts on different multipath signal
3. Time dispersion (echoes) caused by multipath propagation delays

The causes of multipath propagation are reflection, diffraction and scattering. Let us consider them one by one and have an elaboration of them.

2.3.1 Reflection

Reflection occurs when an electromagnetic signal encounters a surface that is large relative to the wavelength of the signal. For example, suppose a ground-reflected wave is received at a receiver. Because the ground-reflected wave has a 180° phase shift after reflection, the ground wave and the LOS wave may tend to cancel, resulting in high signal loss. On the other hand, the reflected signal has a longer path, which creates a phase shift due to delay relative to the unreflected signal. When this delay is equivalent to half a wavelength, the two signals are back in phase. The reflected waves may interfere constructively or destructively at the receiver.

2.3.2 Diffraction

Diffraction occurs at the edge of an impenetrable body that is large compared to the wavelength of the radio wave. When a radio wave encounters such an edge, waves propagate in different directions with the edge as the source. Thus, signals can be received even when there is no unobstructed LOS from the transmitter.

2.3.3 Scattering

If the size of the signal is of the order of the wavelength of the signal or less, scattering occurs. An incoming signal is scattered into several weaker outgoing signals. Scattering effects are difficult to predict.

These three factors affect the performance of the system depending upon the local conditions and the movement of the receiver and transmitter. If the LOS is clear between the receiver and the transmitter, then diffraction and scattering has minor effect but reflection may have a significant impact. If there is no clear LOS available then diffraction and scattering will have significant impact [22].

2.4 Channel Modeling

In 1987 Saleh-Valenzuela gave a channel model based on measurements utilizing low power Ultra-short pulses of width 10ns and center frequency 1.5 GHz in medium-size, two storey building. In this model he assumed that, multipath components arrive at the receiver in

groups (clusters). The arrival of these clusters are assumed to be Poisson distributed with Λ . Within each cluster, the arrival of the multipath components is also assumed to be Poisson distributed with $\lambda > \Lambda$. In this modeling, the channel impulse response is given by [24]

$$h(t) = \sum_{l=0}^{\infty} \alpha_l \delta(t - \tau_l) \quad (2.7)$$

$$= \sum_{l=0}^{\infty} \sum_{n=0}^{\infty} \alpha_{m,n} e^{j\theta_{m,n}} \delta(t - T_{m,n} - \tau_{m,n}) \quad (2.8)$$

$\alpha_{m,n}$ denotes the gain of the n^{th} multipath component of the m^{th} cluster, having phase $\theta_{m,n}$. $T_m + \tau_{m,n}$ ($\tau_{m,0} = 0$) denotes the arrival time of the n^{th} component of the m^{th} cluster, $\theta_{m,n}$ are independent uniform random variable over $[0, 2\pi]$ and $\alpha_{m,n}$ are independent Rayleigh random variable

In 2002, the channel modeling subcommittee of the IEEE 802.15.3a Task group recommended a channel model, which includes aforementioned work as well as recent advancements. According to this new model which is nothing but modified version of Saleh-Valenzuela model, the total number of paths is defined as the number of multi-path arrivals with expected power within 10dB from that of the strongest arrival. In this model Rayleigh distributed model parameter α_l is replaced by log-normal distribution. The phase $\theta_{m,n}$ are also constrained to take values 0 or π , with equal probability to account for signal inversion due to reflection, yielding a real valued channel model.

Let $p(t)$ denote the transmitted pulse of duration T_p . $S_i = \{p_1, p_2, \dots, p_i\}$ After multipath propagation the received waveform $g(t)$ is given by

$$g(t) = p(t) \otimes h(t) \quad (2.9)$$

$$= \sum_{l=0}^{\infty} \alpha_l p(t - \tau_l) \quad (2.10)$$

$$= \sum_{m=0}^{\infty} \sum_{l=0}^{\infty} \alpha_{m,n} e^{j\theta_{m,n}} p(t - T_m - \tau_{m,n}) \quad (2.11)$$

Where \otimes denotes the convolution sign. The spacing among multipath delays $\{\tau_l\}_{l=0}^L$ is in the order of nano seconds. These delayed copies of $p(t)$ can be resolved in $g(t)$ if T_p is sufficiently small.

2.5 Multiple Access Schemes

An efficient multiple access schemes are crucial in this proposed UWB system where multiple signals would overlap in time, frequency and space. Time-Hopping (TH) and Direct-Sequence (DS) are the most popular and simple schemes deployed by UWB systems, as shown in Figure 2.5 [2]. In TH-UWB system, each link is assigned a different periodic time hopping code for multiple access, which introduces a time offset on generated pulses. The time hopping code can also reduce the effect of collisions in multiple access schemes and smooth the PSD of transmitted signals. DS-UWB systems assign a different spreading code to each user which amplitude modulates basic pulses.

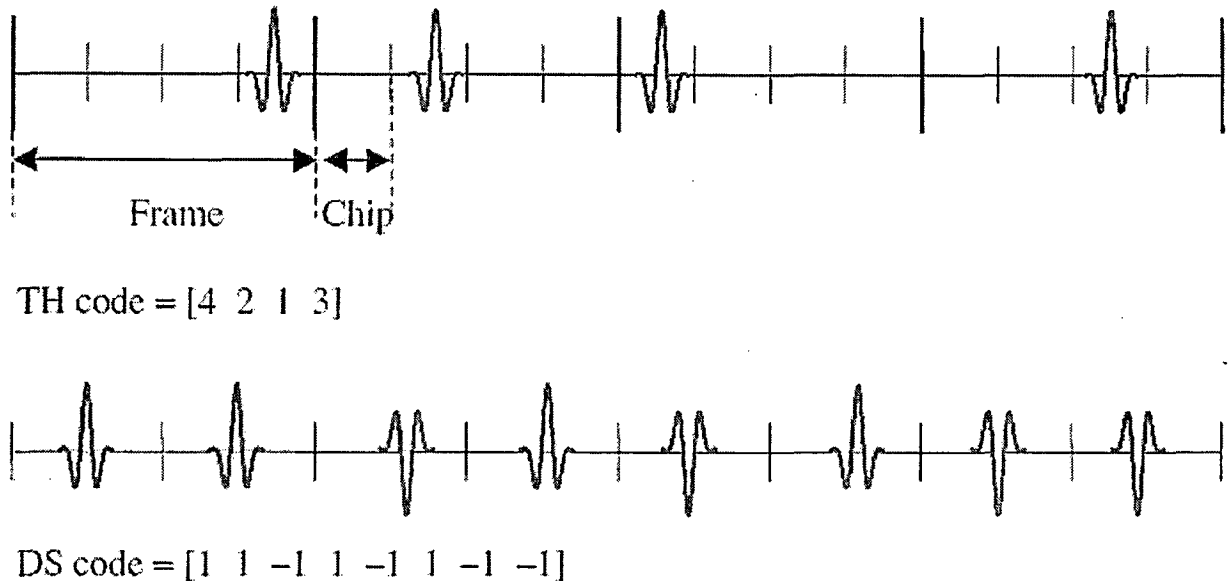


Figure 2.5 TH and DS-UWB-IR Signaling Structure.

CHAPTER 3

RAKE Receiver

3.1 Introduction

Multipath is a common phenomenon which is depicted during the transmission of wireless signals. In this process the transmitted signal proceeds towards its receiver along multiple routes while reflecting, scattering and dispersing due to obstacles it encounters in its path. The receiver in return hears echoes having, in general, different and randomly varying delays and amplitudes.

To overcome the problems created by the multipath, RAKE receiver's concept was evolved and in March 1958 it was presented by R. Price and P. E. Green in their paper [25]. The RAKE receiver is so named because of its analogous function to a garden RAKE, each finger collects bit or symbol energy similarly like tines on a rake collects leaves.

These days RAKE receivers are in widespread use, especially in CDMA systems employing spread spectrum techniques. In these systems the link improvement is obtained through time diversity. Spread spectrum systems are not only resistant to multipath fading but they can also exploit the delayed multipath components to improve the performance of the system. The RAKE receiver anticipates the multipath propagation delays of the transmitted spread spectrum signal and combines the information obtained from the various resolvable multipath components to form a stronger version of the signal [25]. A RAKE receiver consists of a bank of correlators, each of which correlate to a particular multipath component of the desired signal. The Performance Evaluation of RAKE Receivers using Ultra wideband Multipath Channels correlators outputs may be weighted according to their relative strengths and summed to obtain the final signal estimate.

In other word, RAKE receiver as a radio receiver designed to encounter the effects of multipath fading. It does this by using several sub receivers each delayed slightly in order to make it coherent to the individual multipath components. In this process, each component is decoded individually and independently and at a later stage combined in order to make the most use of the different transmission characteristics of each transmission path. This could well result in higher signal to noise ratio, in a multipath communication scenario.

3.2 Diversity and Rake Receiver

The multi-path affected received signal $r(t)$ consists of the superimposition of several attenuated, delayed and eventually distorted replicas of a transmitted waveform $y_m(t)$. When propagation fluctuations within an observation time $T \gg T_b$ and pathdependent distortions can be neglected, $r(t)$ can be expressed as follows:

$$r(t) = \sum_j a_j y_m(t - \tau_j) + n(t) \quad (3.1)$$

where $n(t)$ is the AWGN at the receiver input.

Equation (3.1) can be rewritten for UWB transmissions on the basis of the statistical channel model as.

$$r(t) = X \sqrt{E_{TX}} \sum_j \sum_{n=1}^N \sum_{k=1}^{K(n)} \alpha_{n,k} a_j p_0(t - jT_s - \varphi_j - \tau_{n,k}) + n(t) \quad (3.2)$$

Where

- X is the log-normal distributed amplitude gain of the channel
- E_{TX} is the transmitted energy per pulse
- N is the number of clusters observed at destination
- $K(n)$ is the number of multi-path contributions associated with the n_{th} cluster
- $\alpha_{n,k}$ is the channel coefficient of the k_{th} path within the n_{th} cluster
- a_j is the amplitude of the j_{th} transmitted pulse
- T_s is the average pulse repetition period
- φ_j is the time dithering associated to the j_{th} pulse
- $\tau_{n,k}$ is the delay of the k_{th} path within the n_{th} cluster

The energy contained in the channel coefficients $\alpha_{n,k}$ is normalized to unity for each realization of the channel impulse response, that is:

$$\sum_{n=1}^N \sum_{k=1}^{K(n)} |\alpha_{n,k}|^2 = 1 \quad (3.3)$$

And equation (3.2) can be rewritten as follow

$$r(t) = \sqrt{E_{RX}} \sum_j^N \sum_{n=1}^{K(n)} \alpha_{n,k} a_j p_0(t - jT_s - \varphi_j - \tau_{n,k}) + n(t) \quad (3.4)$$

Where $E_{RX} = X^2 E_{TX}$ is the total received energy for one transmitted pulse. Different from the AWGN channel, E_{RX} is spread in time over the different multi-path contributions and can be used by the detector if the receiver is capable of capturing all replicas of the same pulse. Realistically, the receiver can only analyze a finite subset of N_R contributions and the effective energy E_{eff} , which is used in the decision process, is smaller than E_{RX} , that is

$$E_{eff} = E_{RX} \sum_{j=1}^{N_R} |\alpha_j|^2 \leq E_{RX} \quad (3.5)$$

According to equation (3.4), different replicas of the same transmitted pulse overlap at the receiver only when the corresponding inter-arrival time is smaller than pulse duration T_M . In this case, signals associated with different paths are not independent, that is, the amplitude of the pulse observed at time t is affected by the presence of multi-path contributions arriving immediately before or after time t . Given the characteristics of the propagation channel, the number of independent paths at the receiver depends on T_M : the smaller T_M , the higher the number of independent contributions at the receiver input. For IR-UWB systems, the T_M value is on the order of nanoseconds or fractions of nanoseconds, leading to the hypothesis that all multi-path contributions are non-overlapping, so that the received waveform consists of several independent components [26]. UWB-IR systems can thus principle take advantage of multi-path propagation by combining a large number of different and independent replicas of the same transmitted pulse. In this case, we say that the receiver exploits temporal diversity of the multi-path channel to improve performance of the decision process.

3.4 Common Diversity Techniques

For the combination of different shifted, delayed and attenuated received signals at the RAKE's fingers and for the determination of the desired signal, different diversity techniques are used. The most commonly used of them are:

1. Selection Diversity (SD)
2. Maximal ratio combining (MRC)

3. Equal gain combining (EGC)
4. Minimum mean square error (MMSE)

Let us have a look at each of these techniques

3.4.1 Selection Diversity (SD)

With the SD method, the receiver selects the multi-path contribution exhibiting the best signal quality and operates the decision on the transmitted symbol based on the observation of this contribution only. Choosing the best path guarantees an increase in receiver performance with respect to the simple selection of the first path, deriving from having selected the path with highest instantaneous SNR.

3.4.2 Maximal Ratio Combining

The method of MRC was first proposed by Kahn [23]. In MRC, the different contributions are weighted before the combination and the weights are determined to maximize the SNR before the decision process. In the presence of Gaussian noise at the receiver, the SNR is maximized by applying to each multi-path contribution a weighting factor that is proportional to the amplitude of the corresponding received signal. In other words, the MRC method adjusts the received contributions before combining them. The adjustment is performed by amplifying the strongest components and by attenuating the weak ones. In a single-user communication system without ISI, the method that achieves the best performance is the MRC, which ensures the largest SNR at the combiner output.

3.4.2 Equal Gain Combining

Sometimes, the variable weighting capability for the MRC is not convenient to provide. In this condition all the branch weights are set to 1 or unity but, the signals from each branch are co-phased to provide equal gain combining diversity. The benefit of using this type of diversity is that it allows the receiver to exploit the signals that are received simultaneously on each branch. This dictates that the possibility of producing an acceptable signal from a number of unacceptable input signals is still retained and the performance is marginally inferior to maximal ratio combining [23].

It has been pointed out by [13] that under conditions often occurring in practice, equal-gain systems will perform almost as well as maximal-ratio systems and this fact is of great practical importance.

3.4.3 Minimum Mean Square Error Combining

Pateros and Saulnier studied an adaptive correlator receiver for a DS-SS system employing BPSK signalling in a single user, time-invariant, multipath environment that has a continuum of multipaths but causes no significant ISI [27]. They found that an MMSE receiver detected the transmitted data, removed interference and coherently combined multipaths in the presence of interference undergoing a static single-path channel.

A detector employing MMSE combining technique is the best that we can have for any linear detectors. Multipath signals are employed in a receiver for the detection of the signal. Weights for each path are chosen to give Minimum of the Mean Square Error (MMSE) between the combined voltage stream and the signal.

A major advantage of the MMSE scheme, relative to other interference suppression schemes, is that explicit knowledge of interference parameters is not required [27]. The received signal can be sampled at the pulse repetition frequency after passing through the correlation receiver and the samples are linearly combined using the MMSE criterion, so that the weights are chosen to suppress the NBI.

3.5 Working of RAKE Receiver

In all the above cases, the receiver takes advantage of multi-path under the hypothesis that different replicas of the same transmitted pulse can be analyzed separately and eventually combined before decision. The optimum correlator for the present case must include additional correlators associated with different replicas of a same transmitted waveform. Such a scheme was invented by [25] and is called the RAKE receiver, see figure 3.1.

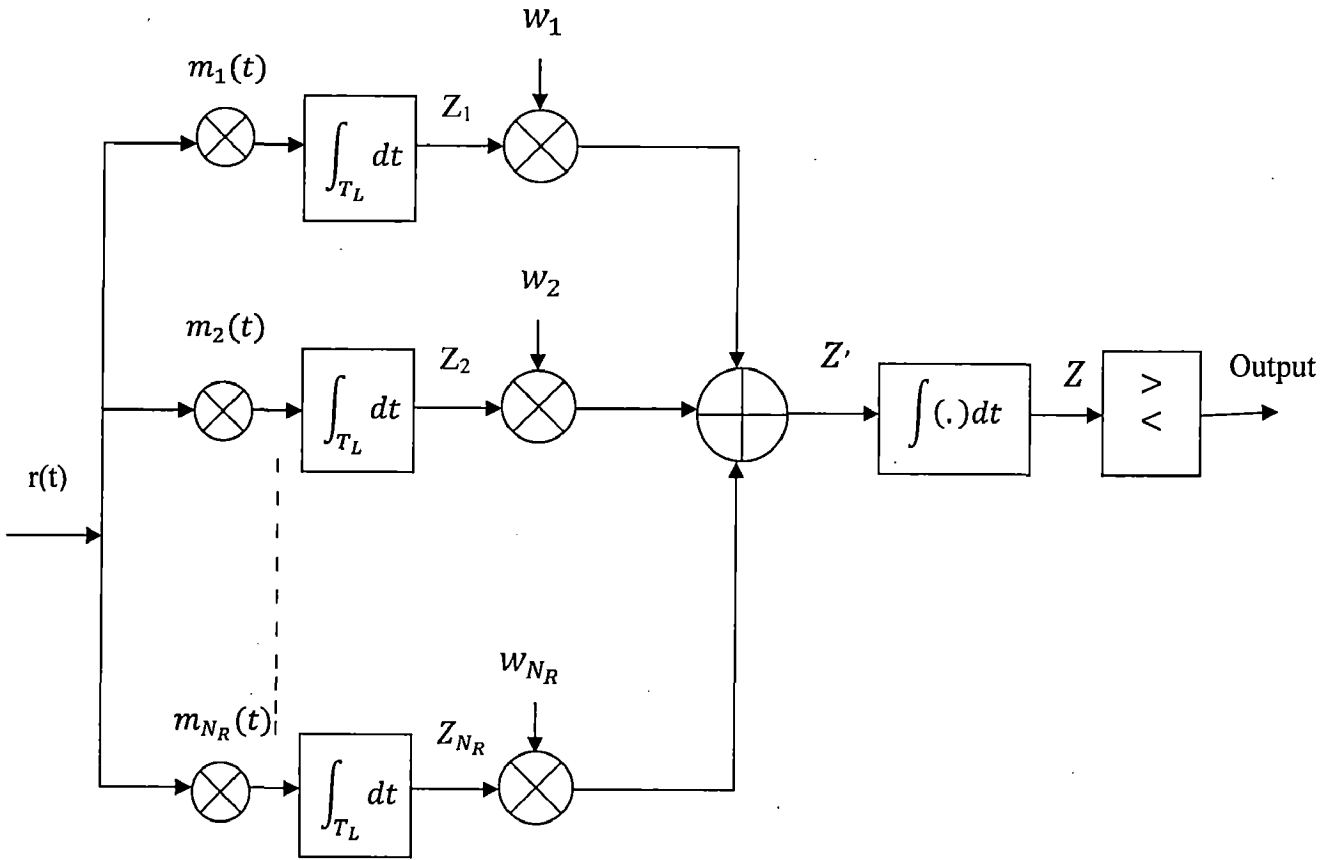


Figure 3.1 Rake Receiver with N_R Parallel Correlators.

In figure 3.1, T_L represents the time duration of the channel impulse response, and z' is the decision variable at the output of the RAKE combiner that enters the detector. Figure 3.1 shows the structure of the RAKE receiver, which consists of a parallel bank of N_R correlators, followed by a combiner that determines the variable to be used for the decision on the transmitted symbol. Each correlator is locked on one of the different replicas of the transmitted symbol, that is, the correlator mask $m_j(t)$ on the j_{th} branch of the RAKE is aligned in time with the j_{th} delayed replica of the transmitted symbol, or:

$$m_j(t) = m(t - \tau_j) \quad (3.6)$$

where $m(t)$ is the correlator mask and τ_j is the propagation delay that characterizes the j_{th} path. The output of the bank of correlators feeds the combiner. Depending on the diversity method implemented at the receiver, a different set of weighting factors $\{w_1, w_2, \dots, w_{N_R}\}$ is used to combine the outputs of the correlators. In the SD case, the weighting factors are equal to zero,

except for the factor on the branch corresponding to the signal with highest amplitude, which is equal to one. In the case of EGC, all factors are equal to 1, that is, the combiner simply adds the outputs of the correlators without applying any weighting. In the MRC case, the output of each branch is multiplied by a weighting factor, which is proportional to the signal amplitude on that branch. Finally, in the MMSE case, Weights for each path are chosen to give Minimize the Mean Square Error (MMSE) between the combined voltage stream and the desired signal.

An alternative but equivalent implementation of the RAKE receiver is shown in Figure 3.2, where the N_R correlators are preceded by time shift elements. The function of these elements is to align all multi-path contributions in time. The advantage of the solution of Figure 3.2 with respect to the schemed of the Figure 3.1 is in the possibility of adopting the same correlator mask $m(t)$ on all branches of the RAKE.

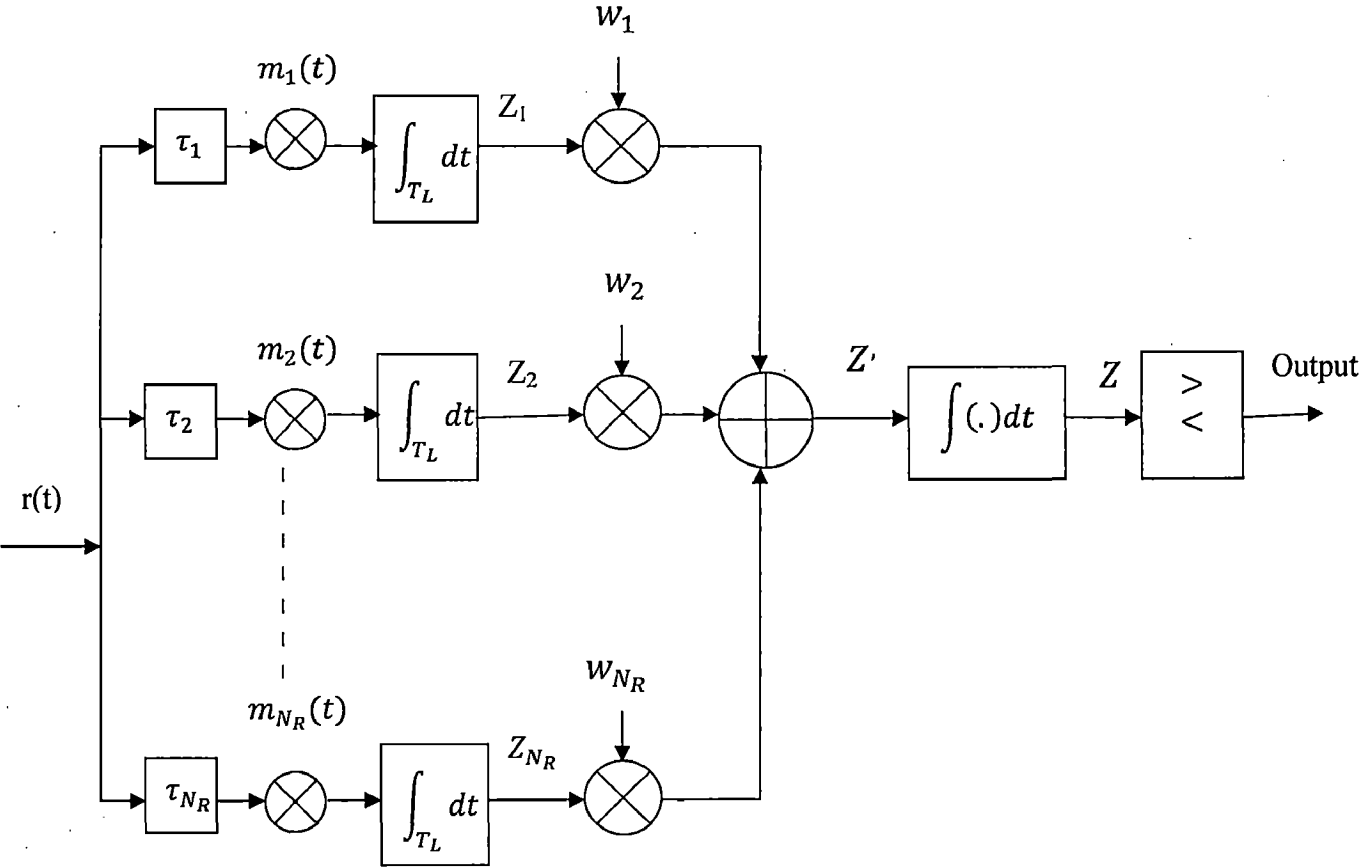


Figure 3.2 Rake Receiver with N_R Parallel Correlators and Time Delay Unit

According to the schemes of Figure 3.1 and 3.2, the RAKE receiver must know the time distribution for all multi-path contributions composing the received waveform. This task is performed by supplying the RAKE with the capability of scanning the channel impulse response, tracking and adjusting the delay of a certain number of multipath components. Time delay synchronization for the different multi-path contributions is based in general on correlation measurements that are performed on the received waveform. In addition, if the SD or MRC methods are adopted within the combiner, the knowledge of the amplitudes of the multi-path component is also required for adjusting the weighting factors. This task is performed in general by using pilot symbols for channel estimation.

The RAKE scheme of Figure 3.2 can be greatly simplified when the channel is modeled with a discrete time impulse response. In this case, the different contributions at the receiver are spaced in time by a multiple of the bin duration ∇t and a single correlators structure is possible for the RAKE, see Figure 3.3. In Figure 3.3, the correlators integrates the product between $m(t)$ and the received waveform $r(t)$. The output of the correlator is sampled with period ∇t before passing through a delay unit and a combiner, which implements one of the previously described diversity methods: SD, EGC, MRC or MMSE.

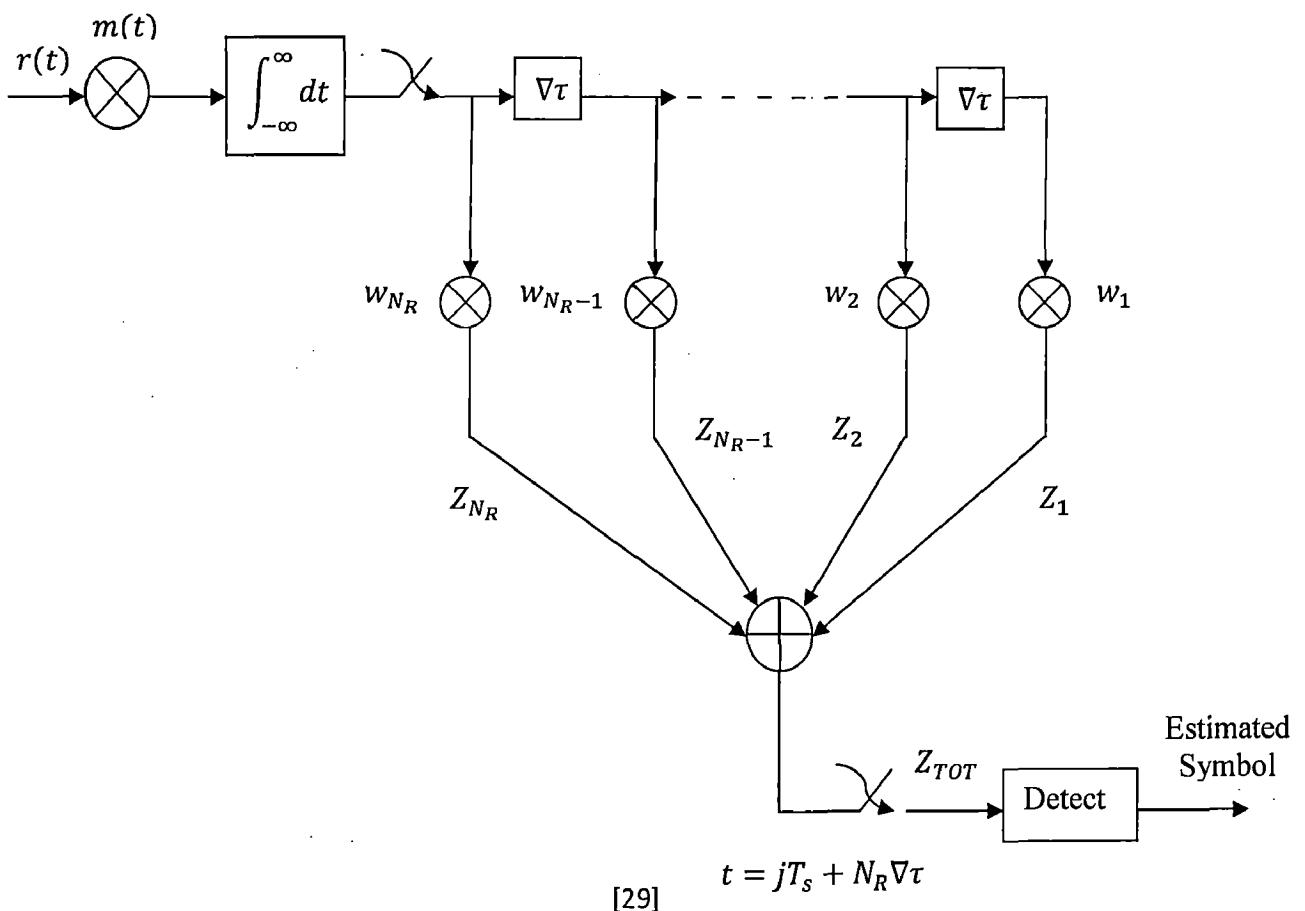


Figure 3.3 RAKE Receiver for Discrete-Time Channel

Performance of the RAKE receiver for propagations over a multi-path channel can be evaluated by first assuming a specific model for the channel impulse response and by then evaluating the probability of error on the symbol P_{r_e} as a function of the E_{RX}/N_0 ratio for the different diversity methods. Here N_0 is half sided PSD of AWGN. This analysis is performed in general under the hypothesis of perfect knowledge of the coefficients of the channel impulse response, or perfect channel estimation.

The adoption of a RAKE considerably increases the complexity of the receiver. This complexity increase with the number of multi-path components analyzed and combined before decision and can be reduced by decreasing the number of components processed by the receiver. According to equation (3.5), however, a reduction of the number of paths leads to a decrease of energy collected by the receiver. A quasi analytical investigation of the existing tradeoff between receiver complexity and percentage of captured energy in a RAKE receiver for IR-UWB systems is presented in [28]. The results of this analysis show that a RAKE receiver operating in a typical modern office building requires about 50 different RAKE branches to capture about 60% of the total energy of the received waveform. In [28], different strategies for reducing the complexity of the RAKE are presented and analyzed in terms of P_{r_e} degradation. The first strategy, called Selective RAKE, consists of selecting the L_B best components among the L_{TOT} available at the receiver input. The number of branches of the RAKE is reduced, but the receiver still must keep track of all the multi-path components to perform the selection. A second and simpler solution, called Partial RAKE, combines the first arriving L_P paths without operating any selecting among all available multi-path components. As expected, Selective RAKE outperforms Partial RAKE since it achieves higher SNR at the output of the combiner. The gap in performance, however, decreases when the best paths are located at the beginning of the channel impulse response as it happens, in general, when considering LOS scenarios.

Chapter 4

The UWB Radio and WLAN Based OFDM Signal

The UWB and Narrowband concepts have been already discussed in Chapter 1. In this chapter, the extension of UWB and Narrowband properties will be examined in more details in terms of mathematical representation as well as real time Matlab generated signals. This chapter also studies the effect of Narrowband onto the UWB in frequency domain.

4.1 UWB Transmitter Structure

A general UWB transmitter block diagram is shown in Figure 4-1 [29].

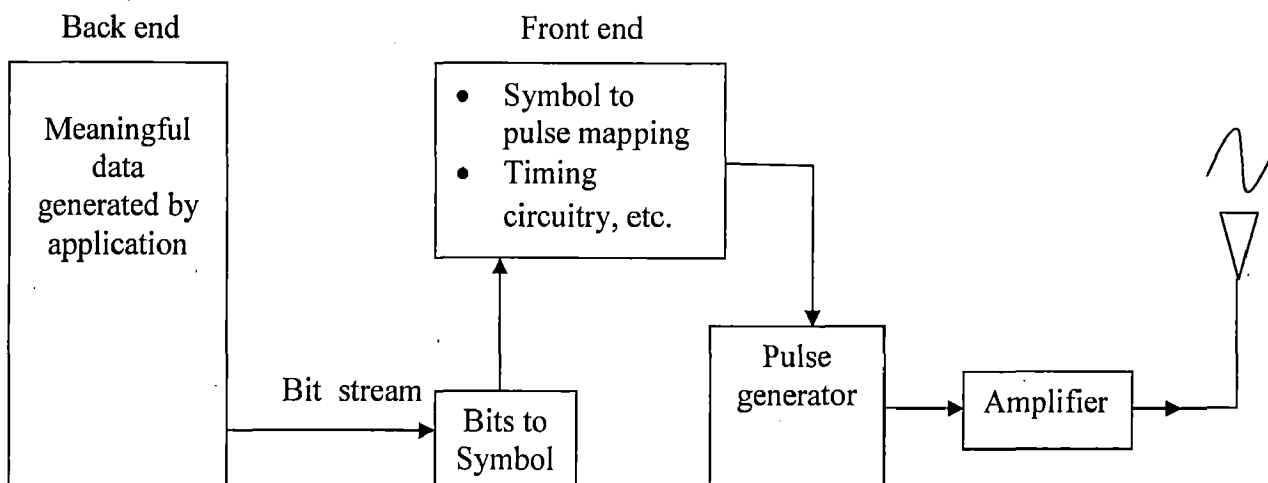


Figure 4-1. A General UWB Transmitter Block Diagram.

First, meaningful data are generated by applications that are separate from the physical layer transmitter. Applications may be an email client or a web browser on a personal computer, a calendar application on a personal digital assistant (PDA), or a digital stream of data from a DVD player. This part of the wireless device is often called the “back end”.

This binary information stream is then passed to the “front end” of the transmitter. If higher modulation schemes are to be used, the binary information are mapped from bits to symbols, each symbol representing multiple bits. These symbols are then mapped onto an analog pulse shape which is generated by a pulse generator. Pulses can be optionally amplified before being passed to an antenna. Large gain of the amplifier is typically not required and may be

omitted since the power spectral of UWB is limited. Precision timing circuitry is required to send the pulses out at specific intervals.

4.2 UWB Receiver Structure

A general UWB receiver block diagram is shown in Figure 4-2. The receiver performs the inverse operations of the transmitter to recover and pass the data to the “back end” applications.

There are two major differences between the transmitter and the receiver. One is that the receiver requires an amplifier to boost the power from the extremely weak received signal. The other is that the receiver must perform the functions of detection or acquisition to locate the desired pulse among the other signals and then continue tracking the desired pulses to compensate any mismatch between the clocks of the transmitter and the receiver.

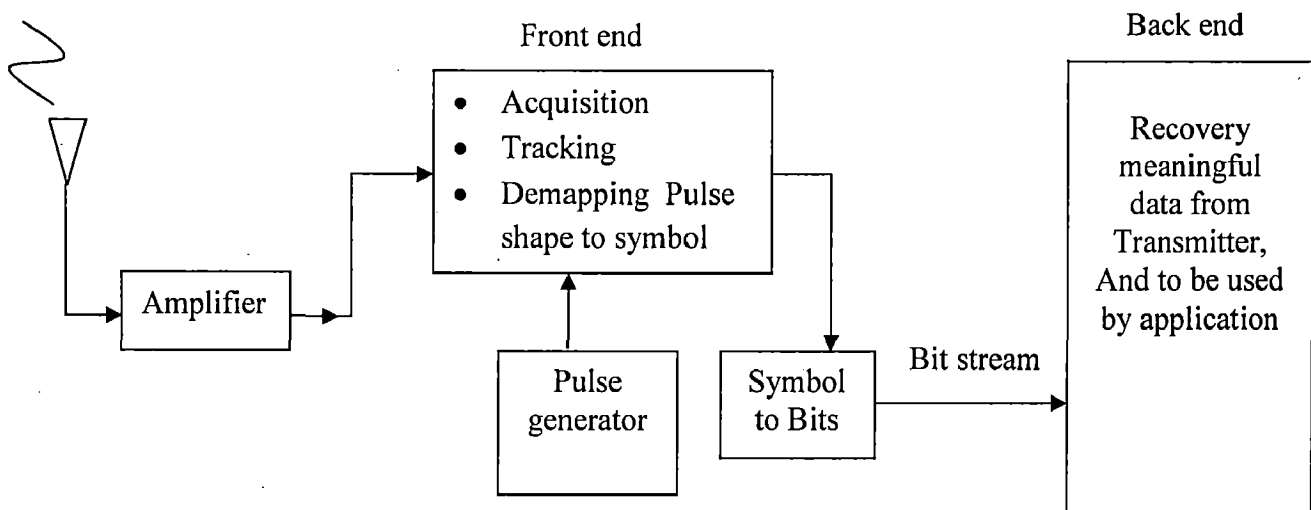


Figure 4-2 A General UWB Receiver Block Diagram.

4.3 Generation of TH-PPM-UWB Signals

The properties of UWB have been already described in Chapter 1 which provide a foundation to build a simple UWB transmitter. The UWB system under investigating is a time-hopping pulse position modulation (TH-PPM-UWB) with a single reference 2nd order derivative Gaussian pulse shape $p(t)$. TH-PPM-UWB is most commonly used in the study of UWB. The system requires only a single template pulse for reception. Most of the complexity of this system

resides in the providing an accurate timing for the generation of the transmitted sequence and subsequent reception. The TH-PPM-UWB signals to be generated can be schematized as shown in Fig 4.3.

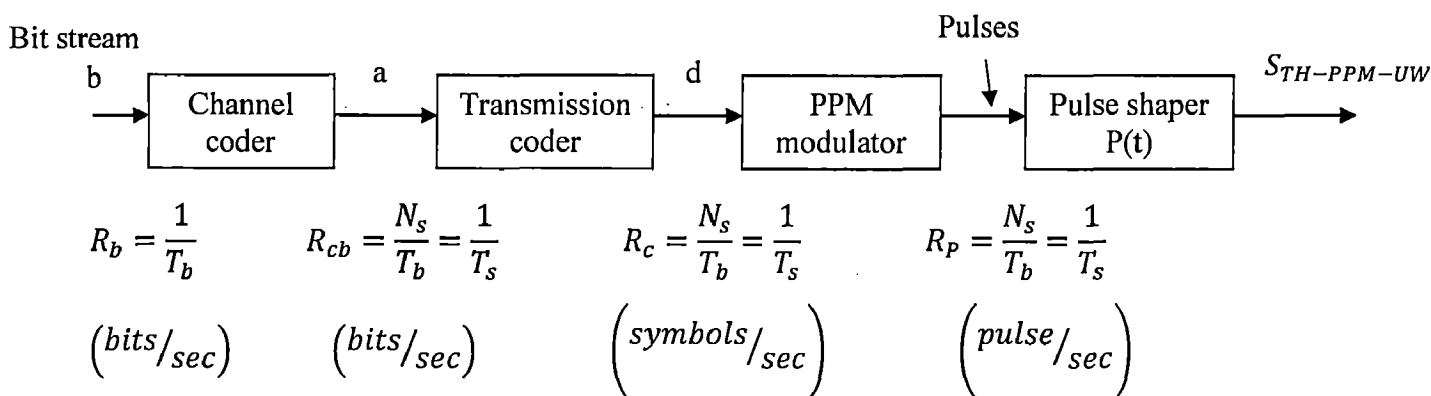


Figure 4.3 Transmission Scheme for a TH-PPM-UWB.

Given the binary sequence $b = (\dots, b_0, b_1 \dots, b_k, b_{k+1} \dots)$, generated at a rate of $R_b = 1/T_b$ bits/s, the first block repeats each bit N_s times and generates a binary sequence $(\dots, b_0, b_0, b_0 \dots, b_1, b_1, b_1 \dots, b_k, b_k, b_k \dots, b_{k+1}, b_{k+1}, b_{k+1} \dots) = (\dots, a_0, a_1 \dots, a_k, a_{k+1} \dots) = a$ at a rate of $R_{cb} = 1/T_b$ bits/s. This system introduces redundancy code is called a block coder indicated as channel coder in the Figure 4.3.

A second block called a transmission coder applies an integer-value code $c = (\dots, c_0, c_1 \dots, c_k, c_{k+1} \dots)$ to the binary sequence $a = (\dots, a_0, a_1 \dots, a_k, a_{k+1} \dots)$ and generates a new sequence d . The generic element of the sequence d is expressed as follows:

$$d_j = c_j T_c + a_j \varepsilon$$

Where T_c and ε are constant terms that satisfy the condition $c_j T_c + \varepsilon < T_s$ for all c_j . In general $\varepsilon < T_c$.

The coded real-valued sequence d enters a third block, the PPM modulator, which generates a sequence of unit pulses (Dirac pulses $\delta(t)$) at a rate of $R_p = N_s/T_b = 1/T_s$ pulses/s.

These pulses are located at time $jT_s + d_j$, and are therefore shifted in time from nominal position jT_s by d_j . Pulses occur at times $(jT_s + c_j T_c + a_j \varepsilon)$ where code c introduces a time hopping (TH) shift on the generated signal.

The last block is a pulse shape filter with impulse response $p(t)$. The impulse response $p(t)$ must be such that the signal at the output of the pulse shaper filter is a sequence of non-overlapping pulses. The most commonly adopted pulse shapes is the second derivatives Gaussian waveform.

The signal $S_{TH-PPM-UWB}(t)$ at the output of the UWB transmitter can be expressed as:

$$S_{TH-PPM-UWB}(t) = \sum_{j=-\infty}^{\infty} p(t - jT_s - c_jT_c - a_j\epsilon) \quad (4.1)$$

The bit interval or bit duration (T_b) is the time used to transmit one bit, the relationship between bit duration and symbol duration expressed as $T_b = N_s T_s$, where N_s is the number of redundant bits. The signal in Equation (4.1) emits two different pulse shapes $p_0(t)$ and $p_1(t)$ in correspondence to the information bits “0” and “1”. The following scenario generated TH-PPM-UWB signal using pseudo random number to generate a set of time-hopping (TH) code with a bit rate of 50 Mbps. In the case of Figure 4.4, the bit stream is [1 0] and the TH code is [2 1 2 2 1] with the time shift introduced by PPM is 0.5 ns and $N_s = 5$.

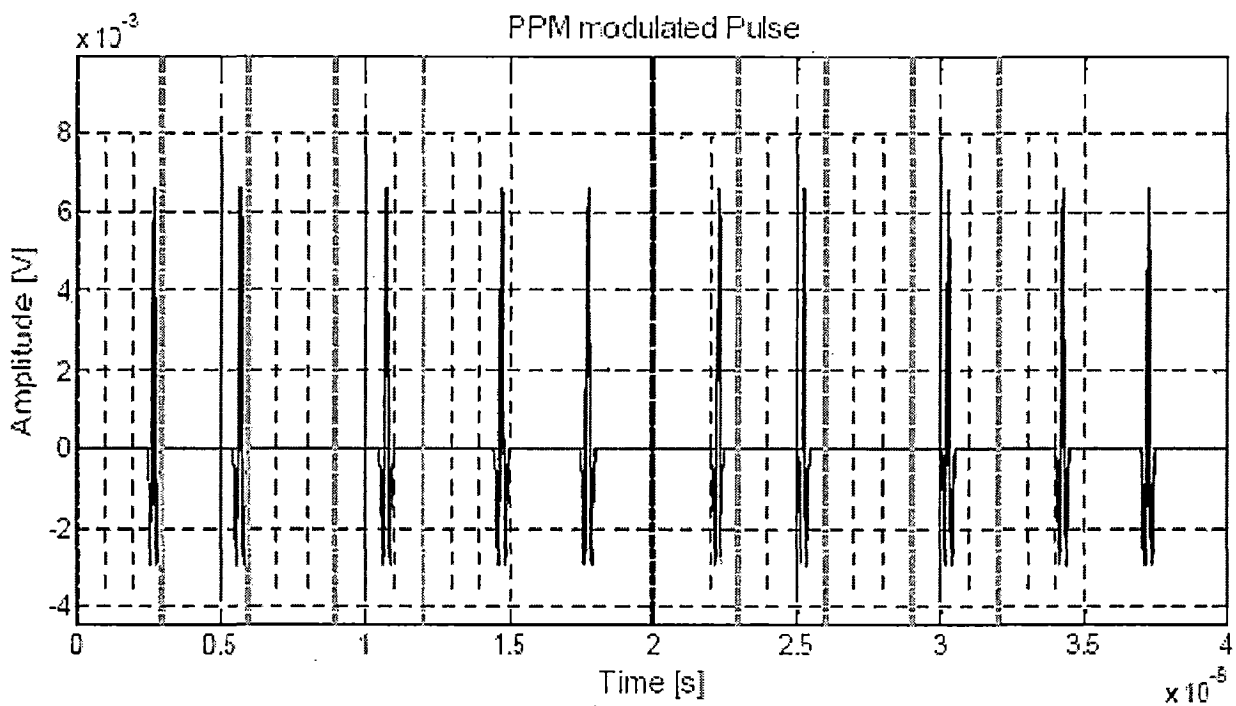


Figure 4.4 TH-PPM-UWB Signal.

4.4 IEEE 802.11a OFDM WLAN Transmitter Structure

A narrowband system consists of a transmitter sending a narrowband signal to a receiver through a dispersive Rayleigh-fading environment.

A typical IEEE 802.11a OFDM WLAN transmitter structure is shown in Fig 4.5 [30]. The stream of complex valued sub-carrier modulation symbols at the output of the mapper is divided into groups of data sub-carrier. Each group is transmitted in an OFDM symbol. All data contains in OFDM symbols is carried by a data carrier and reference information is conveyed in the pilot carriers.

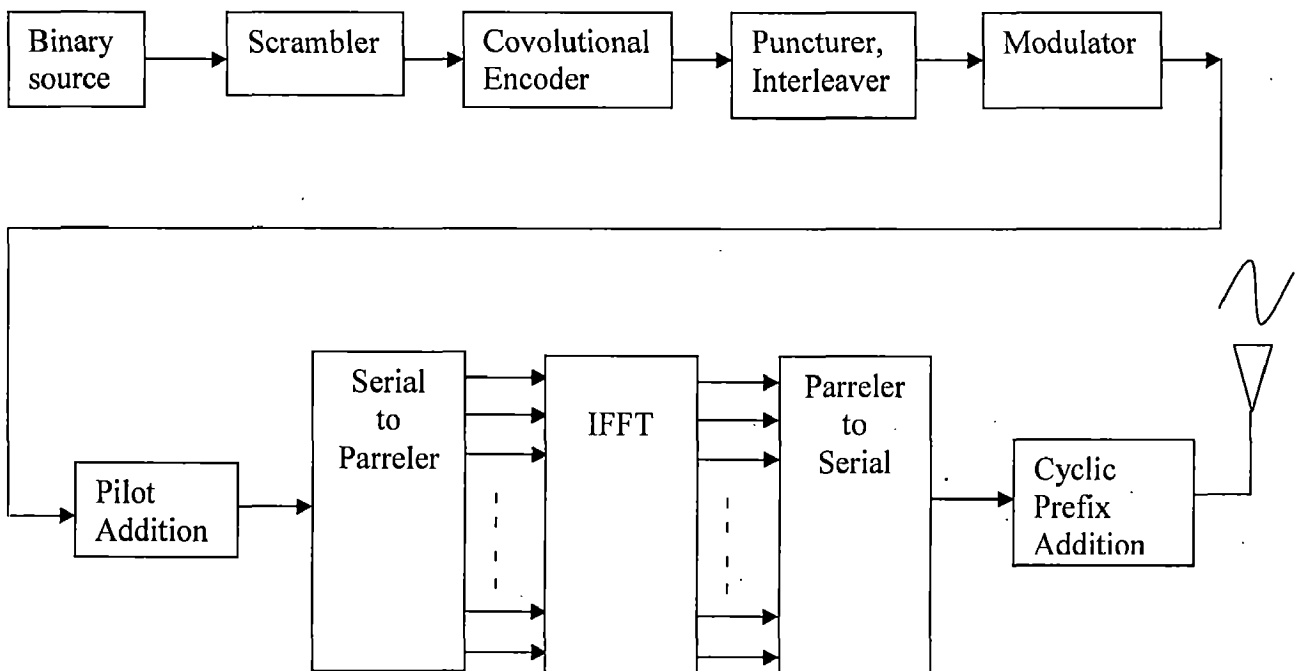


Figure 4.5 Block Diagram of a Typical OFDM Transmitter (IEEE 802.11a Standard)

There are N_{SD} data sub-carriers and N_{SP} pilots sub-carrier for each symbol. Each symbol is constituted by a set of sub-carrier (N_{ST}) and transmitted with a duration T_S . This symbol interval consists of two parts: a useful symbol with duration T_U and a cyclic prefix with duration T_{CP} . The cyclic prefix is a copy of the last T_{CP} / T samples of the symbol part and attached in front of the symbol part when the symbol is sent. Where T is sampling time of OFDM symbol.

4.5 IEEE 802.11a OFDM WLAN Receiver Structure

At the front-end of the receiver, OFDM signals are subject to synchronization errors due to oscillator impairments and sample clock differences. The demodulation of the received radio signal to baseband, possibly via an intermediate frequency, involves 30 oscillators whose frequencies may not be perfectly matched with the transmitter frequencies. This results in a carrier frequency offset.

In addition, demodulation usually introduces phase noise acting as an unwanted phase modulation of the carrier wave. Carrier frequency offset and phase noise degrade performance of the OFDM system. When baseband signals are sampled at the A/D converter, the sample clock frequency at the receiver may not be the same as the one at the transmitter. Not only this sample clock offset causes errors, it also makes duration of an OFDM symbol at the receiver to be different from that at the transmitter. If the symbol clock is taken from the sample clock then variations in the symbol clock will occur. Since the receiver needs to determine when the OFDM symbol begins for proper demodulation with the FFT, a symbol synchronization algorithm at the receiver is usually necessary. Symbol synchronization also compensates for delay changes in the channel.

Channel estimation in OFDM is normally performed with the aid of pilot symbols. Since each subcarrier is flat fading, techniques from single-carrier flat fading systems are directly applicable to OFDM. In OFDM system, the pilot-symbol assisted modulation (PSAM) on flat fading channels involves the sparse insertion of known pilot symbols in the stream of data symbols. Attenuation of the pilot symbols is measured and the attenuations of the data symbols in between these pilot symbols are typically estimated/interpolated using time-correlation properties of the fading channel. After successfully achieving synchronization, the OFDM signals are passed onto the demodulator, de-interleaver and finally to the Viterbi decoder.

4.6 Generation of IEEE 802.11a OFDM WLAN Signals

In general, OFDM system subdivides its available bandwidth into smaller frequency bands. For each sub-band, different types of modulation can be adopted for data transmission and the IR method certainly cannot be applied. The most popular criterion, which has already studied in the IEEE 802.11a is based on the well-known Orthogonal Frequency Division

Multiplexing(OFDM) method. Conceptually, OFDM technique consists of the parallel transmission of several (OFDM) signals that are modulated at different carrier frequencies f_m .

The sequence binary bit stream forms the input of the OFDM modulator is sub-divided into groups of K bits used to generate blocks of N symbols $\{d_0, d_1, \dots, d_m, \dots, d_{N-1}\}$. The generic d_m assumes one of L possible values, which is $K = N \log_2 L$. The symbols are then in turn modulated with different carriers. To transmit the N symbols of a block in parallel, the signals modulating different carriers must be orthogonal in frequency (i.e., the cross products of these carriers are equal to zero). If T_0 is the time used to transmit each symbol on the corresponding carrier, the orthogonality among different transmissions can be achieved by adopting $\Delta f = 1 / T_0$, Where Δf is equally spaced carrier. In addition, a time guard interval T_G is introduced between transmission of the subsequent blocks to prevent Inter-Symbol Interference (ISI). The total OFDM symbol duration is thus $T = T_0 + T_G$ leading to a maximum symbol rate of

$$R_s = \frac{N}{T} = \frac{N}{T_0 + T_G}$$

The length of the guard interval is usually about 20-30% of the total symbol duration T . In general, the guard interval is used to transmit a copy of the final border section of the OFDM symbol. This guard is known as a cyclic prefix. The prefix is introduced to maintain carrier synchronization at the receiver in the presence of time dispersive channels. The length of the cyclic prefix is obviously limited by the duration of the guard interval. At the receiver end, the cyclic prefix is firstly removed.

When comparing the bandwidth of NB, which is about 16 MHz to 3.6 GHz of the UWB, the former bandwidth is extremely small, and thus, NB signal can be treated as a tone in UWB system. The impact of NBI on single user UWB systems was studied in literature review in chapter 1. A DS-SS system is shown to resist NBI from IEEE 802.11a OFDM signals [31], where the NBI was modeled as the multiple access interference (MAI). The use of a maximal ratio combiner (MRC) can suppress MAI but not NBI [12]. BER expressions were derived in [21] for a multi-user time hopping (TH) system operating over a pure AWGN channel (i.e., NBI is not present). These can be used as a benchmark to study the performance of NBI suppression schemes. From [9], The UWB performance affected by NBI is the case when power of NBI is higher compared to the UWB power or both central frequencies are close to each other.

CHAPTER 5

NBI Suppression

5.1 Introduction

The robustness of ultra-wideband (UWB) signals to multipath fading is due to their fine delay resolution, which leads to a high diversity order once combined with a Rake receiver. In order to reduce the Rake complexity while keeping an acceptable system performance, a partial suboptimum Rake receiver, that combines the first arriving paths out of the available resolved multipath components (called PRake), can be used [32].

The performance of a direct-sequence coded division multiple access (DS-CDMA) UWB systems in the presence of NBI has been considered in using a maximal ratio combining (MRC) technique. This combining technique can alleviate the effect of multiple-access interference (MAI) on the system performance, but does not suppress NBI.

Minimum mean square error (MMSE) technique is a well known interference suppression scheme [33]. In this chapter, The performance of time-hopping ultra-wideband (TH-UWB) system is analytically investigated in a UWB realistic multipath channel and in the presence of narrowband interference (NBI). The discussed technique is based on the use of a Rake receiver followed by MMSE combining. After correlation, the received signal is sampled at the pulse repetition frequency. The obtained samples are weighted and linearly combined using the MMSE combining (MMSEC) criterion, so that NBI can be suppressed. Both pulse position modulation (PPM) and pulse amplitude modulation (PAM) schemes are considered. The NBI signal is modeled as a traditional single carrier BPSK modulated waveform. The expressions of the signal-to-interference and noise ratio at the output of the selective Rake combiner, the system multi-access data rate as well as the conditional bit error rate are also derived.

The impact of different parameters, such as the number of selected dominant paths, the NBI power as well as the time hopping sequence code on the system performance are discussed in next chapter through simulation.

5.2 TH-PPM-UWB System Model

The typical TH-UWB transmitted signal can be expressed as

$$S_{tr} = \sum_{j=-\infty}^{\infty} a_{\lfloor j/N_s \rfloor} w_{tr}(t - jT_f - c_j T_c - \delta b_{\lfloor j/N_s \rfloor}) \quad (5.1)$$

- j : indicate frame number
- $w_{tr}(t)$: transmitted Monocycle waveform
- T_f : pulse repetition time
- c_j : Time hopping (TH) Sequence, can take on any value between 0 to $(N_h - 1)$
- N_h : Number of hops
- T_c : chip duration, that satisfy $N_h T_c \leq T_f$

In a typical TH-UWB system, each data symbol is transmitted over multiple monocycles. Denote by N_s the number of pulses that correspond to the information bit, then the symbol rate denoted by R_s , is simply given by $R_s = \frac{1}{N_s T_f}$

Both PPM and PAM modulation have been suggested for TH-UWB systems. In PAM UWB systems the information is conveyed by the series $\{a_{\lfloor j/N_s \rfloor}\}$ where $\lfloor \cdot \rfloor$ denotes the integer part. $\{a_{\lfloor j/N_s \rfloor}\}$ takes on value ± 1 while $b_{\lfloor j/N_s \rfloor} = 0$ for all j . However, in PPM UWB systems the information is conveyed by the series $\{b_{\lfloor j/N_s \rfloor}\}$ which takes value ± 1 while $a_{\lfloor j/N_s \rfloor} = 1$ for all j . The parameter δ is a time shift added to a monocycle when we transmit the bit “+ 1” and subtracted when we transmit the bit “- 1”.

δ is the order of T_m where the monocycle waveform $w_{tr}(t)$ is nonzero only in interval $[0, T_m]$. Modulated data denoted by $d_{\lfloor j/N_s \rfloor}$, where

$$d_{\lfloor j/N_s \rfloor} = \begin{cases} a_{\lfloor j/N_s \rfloor} & \text{for PAM} \\ b_{\lfloor j/N_s \rfloor} & \text{for PPM} \end{cases} \quad (5.2)$$

In this chapter, consider an L multipath component UWB frequency selective channel [34]. The receiving antenna system modifies the shape of the transmitted monocycle $w_{tr}(t)$ to its derivative $w_{rec}(t)$. Many types of pulse shapes have been suggested for TH-UWB systems, among them the second derivative of Gaussian pulse wave use as transmitted monocycle waveform, which are used in the numerical results.

In the receiver side received signal $r(t)$ can be modeled as:

$$r(t) = M(t) + I(t) + n(t) \quad (5.3)$$

Where $M(t)$ is received UWB signal after passing through UWB channel, And expressed as

$$M(t) = \sum_{j=-\infty}^{\infty} a_{|j/N_s|} \sum_{l=0}^{L-1} \alpha_l w_{rec}(t - jT_f - c_j T_c - \delta b_{|j/N_s|} - \tau_l) \quad (5.4)$$

Where,

- α_l denote the fading amplitude over l_{th} propagation path of received UWB signal
- τ_l denote the delay over l_{th} propagation path of received UWB signal

Where NBI term $I(t)$ modeled as a traditional single carrier BPSK modulated waveform, given by

$$I(t) = \sqrt{2P_I} \cos(w_0 t + \theta) \sum_{k=-\infty}^{\infty} g_k z(t - kT_1 - \tau_1) \quad (5.5)$$

Where,

- $z(t)$ is the baseband waveform shape.
- P_I is the average transmitted power of Narrowband waveform.
- $w_0 = 2\pi f_0$, is the carrier frequency of Narrowband waveform.
- θ is the random phase of Narrowband waveform.
- $\{g_k\}$ is the randomly modulated BPSK symbol, where $g_k \in \{\pm 1\}$.
- T_1 is the symbol period.
- τ_1 is random delay, uniformly distributed in $[0, T_1]$.

Finally, the random variable $n(t)$ denotes the received AWGN noise which is modeled as $N(0, \sigma_n^2)$. Where $\sigma_n^2 = \frac{N_0}{2}$ is variance of AWGN noise, And N_0 is half sided power spectral density of AWGN noise.

In the next section, analyze the performance of an innovative MMSE-Rake receiver that is able to suppress the NBI and estimate the desired user transmitted data, $\hat{d}_{|j/N_s|}$.

5.3 MMSE-RAKE Receiver for TH-UWB System

The Rake receiver is widely employed in wideband systems in order to take advantage of the frequency selective channel. Indeed, it resolves the components of the received signal and combines them to provide multipath diversity. The number of combined multipath components in a typical Rake combiner is limited by several factors including the design complexity.

A major advantage of the MMSE scheme, relative to other interference suppression schemes, is that explicit knowledge of interference parameters is not required. In this section, will use a P-Rake receiver based on a bank of correlator fingers followed by an appropriate MMSE technique, as shown in Fig. 5.1 [35].

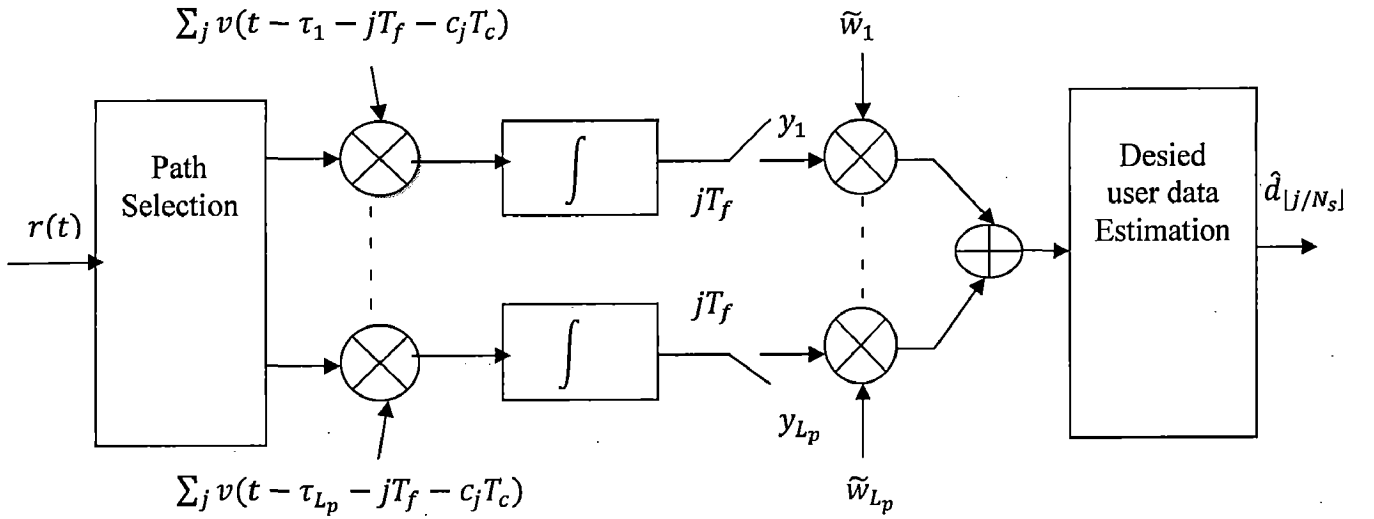


Figure 5.1 MMSE-Rake Receiver Model for TH-PPM-UWB System.

Each correlator branch consists of a summation of the N_s pulse correlations of the received signal with the locally generated correlator's template waveform corresponding to the j_{th} frame of user of interest. The pulse correlator's template, $v_{rec}(t)$, is shifted to different times, the j_{th} template frame normally starting at time $jT_f + c_jT_c + \tau_l$.

Assume that the receiver knows the channel perfectly as well as the time asynchronism between its signal clock and the receiver clock. That is, the receiver is perfectly locked to the signal from user. Then correlation output of each Rake finger is given by

$$y_l = \sum_{j=0}^{N_s-1} \int_{\tau_l + jT_f}^{\tau_l + (j+1)T_f} r(t)v(t - jT_f - c_jT_c - \tau_l)dt \quad (5.6)$$

Where $l = 0, 1, 2, \dots, L_p - 1$. And L_p is number of P-RAKE finger.

where $v(t)$ is the correlator's template signal expressed as

$$v(t) = \begin{cases} w_{rec}(t) & \text{for PAM} \\ w_{rec}(t - \delta) - w_{rec}(t + \delta) & \text{for PPM} \end{cases} \quad (5.7)$$

As $w_{rec}(t)$ is non-zero only in the time interval $[0, T_m]$, the support of the template, $v(t)$, is

$$[T_{v1}, T_{v2}] = \begin{cases} [0, T_m] & \text{for PAM} \\ [-\delta, T_m + \delta] & \text{for PPM} \end{cases} \quad (5.8)$$

The substitution of the received signal expression $r(t)$ from equation (5.3) into the correlator output expression (5.6) yields to

$$y_l = \sum_{j=0}^{N_s-1} \int_{T_{v1}}^{T_{v2}} r(t + jT_f + c_jT_c + \tau_l) v(t) dt \quad (5.9)$$

$$y_l = M_l + I_l + N_l \quad (5.10)$$

Where, M_l denote the output of l correlator finger due to TH-PPM-UWB signal, And its given by

$$M_l = \sum_{j=0}^{N_s-1} \int_{T_{v1}}^{T_{v2}} M(t + jT_f + c_jT_c + \tau_l) v(t) dt \quad (5.11)$$

Likewise, I_l denote the output of l correlator finger due to NBI signal input, And its given by

$$I_l = \sum_{j=0}^{N_s-1} \int_{T_{v1}}^{T_{v2}} I(t + jT_f + c_jT_c + \tau_l) v(t) dt \quad (5.12)$$

And, N_l denote the output of l correlator finger due to AWGN noise input, And its given by

$$N_l = \sum_{j=0}^{N_s-1} \int_{T_{v1}}^{T_{v2}} N(t + jT_f + c_jT_c + \tau_l) v(t) dt \quad (5.13)$$

For develop a closed form expression for the output of the correlator finger, Let define the cross-correlation function between the received monocycle pulse, $w_{rec}(t)$, and the correlator's template signal, $v(t)$ is given by

$$\rho_{(v,w,x)}(\tau) = \begin{cases} \int_{T_{v1}}^{T_{v2}} w_{rec}(u + vT_f + wT_c + xT_m - \tau) v(u) du & , \text{for PAM} \\ \int_{T_{v1}}^{T_{v2}} w_{rec}(u + vT_f + wT_c + xT_m - \tau - \delta) v(u) du & , \text{for PPM} \end{cases} \quad (5.14)$$

Where, v, w and x stand, respectively, for the coefficient of T_f, T_c , and T_m in the argument of the received monocycle pulse $w_{rec}(t)$.

When consider TH-PPM-UWB signal with NBI signal, cross-correlation function between $w_{rec}(t)$ and $v(t)$ takes on a value different from zero if and only if

$$vT_f + wT_c + xT_m = 0 \quad (5.15)$$

i.e

$$\rho_{(v,w,x)}(\tau) = \begin{cases} \int_{T_{v1}}^{T_{v2}} w_{rec}(u - \tau) w_{rec}(u) du & \text{for } vT_f + wT_c + xT_m = 0 \text{ and } \\ \int_{T_{v1}}^{T_{v2}} w_{rec}(u - \tau - \delta) (w_{rec}(u - \delta) - w_{rec}(u + \delta)) du & \text{for } vT_f + wT_c + xT_m = 0 \text{ and } \\ 0 & \text{if } vT_f + wT_c + xT_m \neq 0 \end{cases} \quad (5.16)$$

Using this property of the cross-correlation function between $w_{rec}(t)$ and $v(t)$, the desired and multi-access term M_l can be expressed as

$$M_l = \sum_{j=0}^{N_s-1} d_{\lfloor j/N_s \rfloor} \sum_{l=0}^{L-1} \alpha_l \rho_{(-\beta_{l,l}, 0, Q_{l,l})}(\tau) \quad (5.17)$$

Where the difference between the delays over the l_{th} propagation path of the signal received from the user and the l'_{th} propagation path of the desired user signal can be modeled as

$$\tau_l - \tau_{l'} = \beta_{l,l'} T_f + \mu_{l,l'} \quad (5.18)$$

Here, $\beta_{l,l'}$ is the value of time uncertainty $\tau_l - \tau_{l'}$ rounded to near frame time. And $\mu_{l,l'}$ is the error in this rounding process, is a uniformly distributed random variable over $\left[-T_f/2, T_f/2\right]$.

Since the delay over the l_{th} propagation path of the signal received from the user satisfy $0 \leq \tau_l < N_s T_f$, Where $T_f = N_s T_c$.

so the error in this rounding process $\mu_{l,l'}$ can be approximated as $\mu_{l,l'} = Q_{l,l'} T_m$

Here, $Q_{l,l'}$ is an integer uniformly distributed over the interval $[0, N_h N_c - 1]$, with $N_c = T_c / T_m$.

At the reception, each user, employs a Partial Rake combining receiver composed of L_p correlators corresponding to the L_p selected paths out of the L available paths. Then combined output signal of the Partial Rake receiver can be written as

$$\mathbf{S}_{COMB} = \mathbf{W} (\mathbf{M}_{L_p} + \mathbf{I}_{L_p} + \mathbf{N}_{L_p}) \quad (5.19)$$

$$\mathbf{S}_{COMB} = \mathbf{M} + \mathbf{I} + \mathbf{N} \quad (5.20)$$

Where,

- $\mathbf{M} = \mathbf{W} \cdot \mathbf{M}_{L_p}$, stand for combined output signal of the Partial RAKE receiver due to TH-UWB signal input, Where $\mathbf{M}_{L_p} = [M_0, M_1, \dots, M_{L_p-1}]$.
- $\mathbf{I} = \mathbf{W} \cdot \mathbf{I}_{L_p}$, stand for combined output signal of Partial RAKE receiver due to NBI signal input, Where $\mathbf{I}_{L_p} = [I_0, I_1, \dots, I_{L_p-1}]$.
- $\mathbf{N} = \mathbf{W} \cdot \mathbf{N}_{L_p}$, stand for combined output signal of Partial RAKE receiver due to AWGN noise input, Where $\mathbf{N}_{L_p} = [N_0, N_1, \dots, N_{L_p-1}]$.
- \mathbf{W} is weight coefficient vector, is given by

$$\mathbf{W} = [w_0, w_1, \dots, w_{L_p-1}]$$

Where, w_l for $l = 0, 1, 2, \dots, L_p - 1$, is weight coefficient chosen to minimize the mean square error, is given by

$$MSE = E \left[|d_{|j/N_s|} - w_l y_l|^2 \right] \quad (5.21)$$

Using the property of the cross-correlation function between $w_{rec}(t)$ and $v(t)$, the desired UWB term \mathbf{M} can be expressed as

$$\mathbf{M} = N_s d_{|j/N_s|} \sum_{l=0}^{L_p-1} \sum_{l=0}^{L-1} \alpha_l w_l \rho_{(-\beta_{l,l}, 0, Q_{l,l})}(\tau) \quad (5.22)$$

Hence, the desired user signal energy term is

$$E_D = E[\mathbf{M} \cdot \mathbf{M}] \quad (5.23)$$

$$E_D = N_s^2 \sum_{l=0}^{L-1} |\alpha_l|^2 \left| \sum_{l=0}^{L_p-1} w_l \right|^2 \sigma_{l,l}^2 \quad (5.24)$$

$$\text{Where, } \sigma_{l,l}^2 = \frac{1}{T_f} \int_{-\infty}^{\infty} \rho_{(-\beta_{l,l}, 0, Q_{l,l})}^2(\tau) d\tau$$

As the NBI term is fully contained within the bandwidth of the UWB waveform. The NBI symbol period T_1 is much greater than the monocycle pulse repetition interval T_f . Therefore, due to the limit of the Rake finger delays, the summation over the narrowband modulated symbols can be truncated [12].

There for NBI signal energy term at the output of RAKE receiver is given by

$$E_I = E[\mathbf{I} \cdot \mathbf{I}] \quad (5.25)$$

$$E_I = N_s^2 \left| \sum_{l=0}^{L_p-1} w_l \right|^2 \int_{T_{v1}}^{T_{v2}} \int_{T_{v1}}^{T_{v2}} R_I(t - \tau) v(t) v^*(\tau) dt d\tau \quad (5.26)$$

Where, * denote conjugate and $R_I(\tau)$ denote auto-correlation function of NBI signal and given by

$$R_I(\tau) = \int_{-\infty}^{\infty} I(t) I^*(t + \tau) dt \quad (5.27)$$

Then,

$$E_I = N_s^2 \left| \sum_{l=0}^{L_p-1} w_l \right|^2 E_{Iv} \quad (5.28)$$

Where, $E_{Iv} = \int_{T_{v1}}^{T_{v2}} \int_{T_{v1}}^{T_{v2}} R_I(t - \tau) v(t) v^*(\tau) dt d\tau$

At last the output terms of the Partial Rake combining receiver due to the AWGN noise is, $N = \mathbf{W} \cdot \mathbf{N}_{L_p}$, are i.i.d. Gaussian random variables with zero mean and variance σ_{rec}^2 , where

$$\sigma_{rec}^2 = N_s^2 \frac{N_0}{2} \left| \sum_{l=0}^{L_p-1} w_l \right|^2 \int_{-\infty}^{\infty} v^2(t) dt \quad (5.29)$$

Let $E_v = \int_{-\infty}^{\infty} v^2(t) dt$, Then

$$\sigma_{rec}^2 = N_s^2 \frac{N_0}{2} \left| \sum_{l=0}^{L_p-1} w_l \right|^2 E_v \quad (5.30)$$

In the next section will find optimal weight vector based on MMSE for combat NBI in TH-PPM-UWB system.

5.4 Calculation of the MMSE-Rake Optimal Weights

The weight vector used for combining at the P-Rake receiver is the one that minimizes the Mean-Square Error (MSE) given by

$$MSE = E \left[|d_{j/N_s} - w_l y_l|^2 \right] \quad (5.31)$$

And the optimal MMSE weight vector, w_l , to detect user's j_{th} bit satisfies

$$\tilde{w}_l = \arg \min_{w_l} \left[|w_l| E[|y_l|^2] - 2 \operatorname{Re}(w_l E[d_{j/N_s} y_l]) \right] \quad (5.32)$$

Using the expression for y_l , given in eq. (8), The quantity $E[|y_l|^2]$ can be re-written as

$$E[|y_l|^2] = E_D + E_I + \sigma_{rec}^2 \quad (5.33)$$

Using eqs

$$E[|y_l|^2] = N_s^2 \left(\sum_{l=0}^{L-1} |\alpha_l|^2 \left| \sum_{l=0}^{L_p-1} w_l \right|^2 \sigma_{l,l}^2 + \left| \sum_{l=0}^{L_p-1} w_l \right|^2 E_{Iv} + \frac{N_0}{2} \left| \sum_{l=0}^{L_p-1} w_l \right|^2 E_v \right) \quad (5.34)$$

Where,

$$\sigma_{l,l}^2 = \frac{1}{T_f} \int_{-\infty}^{\infty} \rho_{(-\beta_{l,l}, 0, Q_{l,l})}^2(\tau) d\tau \quad (5.35)$$

And the quantity $E[d_{j/N_s} y_l]$ can be wirtten as

$$E[d_{j/N_s} y_l] = N_s \rho_{(0,0,0)}(\tau) \alpha_l \quad (5.36)$$

Thus, the optimal weight that minimizes the MSE is given by

$$\tilde{w}_l = \frac{\rho_{(0,0,0)}(\tau) \alpha_l}{N_s \left(\sum_{l=0}^{L-1} |\alpha_l|^2 \left| \sum_{l=0}^{L_p-1} w_l \right|^2 \sigma_{l,l}^2 + \left| \sum_{l=0}^{L_p-1} w_l \right|^2 E_{Iv} + \frac{N_0}{2} \left| \sum_{l=0}^{L_p-1} w_l \right|^2 E_v \right)} \quad (5.37)$$

or in simple way, can say [27]

$$\tilde{w}_l = \frac{\rho_{(0,0,0)}(\tau) \alpha_l}{(R_S + R_I + R_N)} \quad (5.38)$$

Where, R_S , R_I , and R_N are respectively, the autocorrelation of the signal, the NBI and the noise.

5.4 System Average Bit Error Rate

For evaluation BER of system, considering indoor environment, the fading is assumed to be sufficiently slow that a large number of bits are transmitted essentially over the same channel. In this case and in order to easily evaluate the system performance, a numerical method is considered to average the conditional BER conditioned on the channel conditions, the characteristics of the used MMSEC-Rake and the parameters of NBI.

Let the expression for desired UWB term, \mathbf{M} can be re-written as

$$\mathbf{M} = a_{\lfloor j/N_s \rfloor} \sum_{l=0}^{L_p-1} \sum_{l=0}^{L-1} \alpha_l w_l \rho_{(-\beta_{l,l}, 0, Q_{l,l})}(\tau) \quad (5.39)$$

For simplicity, Let define desired UWB signal vector

$$\mathbf{D} = [D_{l_0}, D_{l_1}, \dots, D_{l_{L_p-1}}]^T \quad (5.40)$$

Where,

$$D_l = \frac{1}{\sqrt{P}} a_{\lfloor j/N_s \rfloor} \sum_{l=0}^{L-1} \alpha_l \rho_{(-\beta_{l,l}, 0, Q_{l,l})}(\tau) \quad (5.41)$$

Here, P is the average transmit power of the UWB signal and its given by

$$P = B_S \int_0^{T_c} E[s_{tr}^2(t)] dt \quad (5.42)$$

And B_S is the occupied bandwidth of the transmitted waveform.

Using the above equation the output of the Partial Rake receiver due to UWB signal input can be written as

$$\mathbf{M} = \frac{\sqrt{P}}{B_S} \mathbf{W} \cdot \mathbf{D} \quad (5.43)$$

And the received NBI term signal vector can be written as

$$\mathbf{I}_{NBI} = \frac{B_S}{\sqrt{P_t}} \mathbf{I} \quad (5.44)$$

Here, P_t is the total NBI average power.

The combined output of the Partial Rake receiver can be written as follows:

$$\mathbf{S}_{COMB} = \mathbf{M} + \mathbf{I} + \mathbf{N} \quad (5.45)$$

$$\mathbf{S}_{COMB} = \frac{\sqrt{P}}{B_S} \mathbf{W} \cdot \mathbf{D} + \frac{\sqrt{P_t}}{B_S} \mathbf{W} \cdot \mathbf{I}_{NBI} + \mathbf{W} \cdot \mathbf{N} \quad (5.46)$$

Here, \mathbf{S}_{COMB} is a conditional Gaussian random variable conditioned on the channel conditions, the characteristics of the MMSEC-Rake used, NBI parameters. The conditional mean of \mathbf{S}_{COMB} is $\mathbf{M} + \mathbf{I}$ and its variance is σ_{rec}^2 as given in eq (5.29).

Therefore, the TH-UWB conditional Bit error rate (theoretical) is

$$BER_{COND} = Q \left[\frac{\sqrt{\frac{2E_b}{N_s N_0}} W \cdot D + \sqrt{\frac{P_t}{P}} W \cdot I_{NBI}}{\sqrt{|\sum_{l=0}^{L-1} w_l|^2 N_s^2 E_v}} \right] \quad (5.47)$$

Here, $Q[.]$ denotes as Q-function, that is define as

$$Q[Z] = \int_z^{\infty} \frac{1}{\sqrt{2\pi}} \exp\left(-y^2/2\right) dy \quad (5.48)$$

And from eq. (5.24), (5.28) and (5.30), signal to noise plus interference ratio is define as

$$SNIR = \frac{E_D}{E_I + \sigma_{rec}^2} \quad (5.49)$$

And signal to noise ratio is

$$SNR = \frac{E_D}{\sigma_{rec}^2} \quad (5.50)$$

Chapter 6

Simulation Results and Discussion

In this chapter, first the simulation set-up is described and followed with the simulation results. The chapter ends with analysis and discussion of the simulation and its results.

6.1 Simulation Set-up

MATLAB was used to generate the UWB signal $w_{tr}(t)$ and the Narrowband signal $I(t)$ presented in Chapter 4. And also used to construct a MMSE-RAKE receiver as described in Chapter 3. The block diagram of the simulation is shown in Figure 5-1 below.

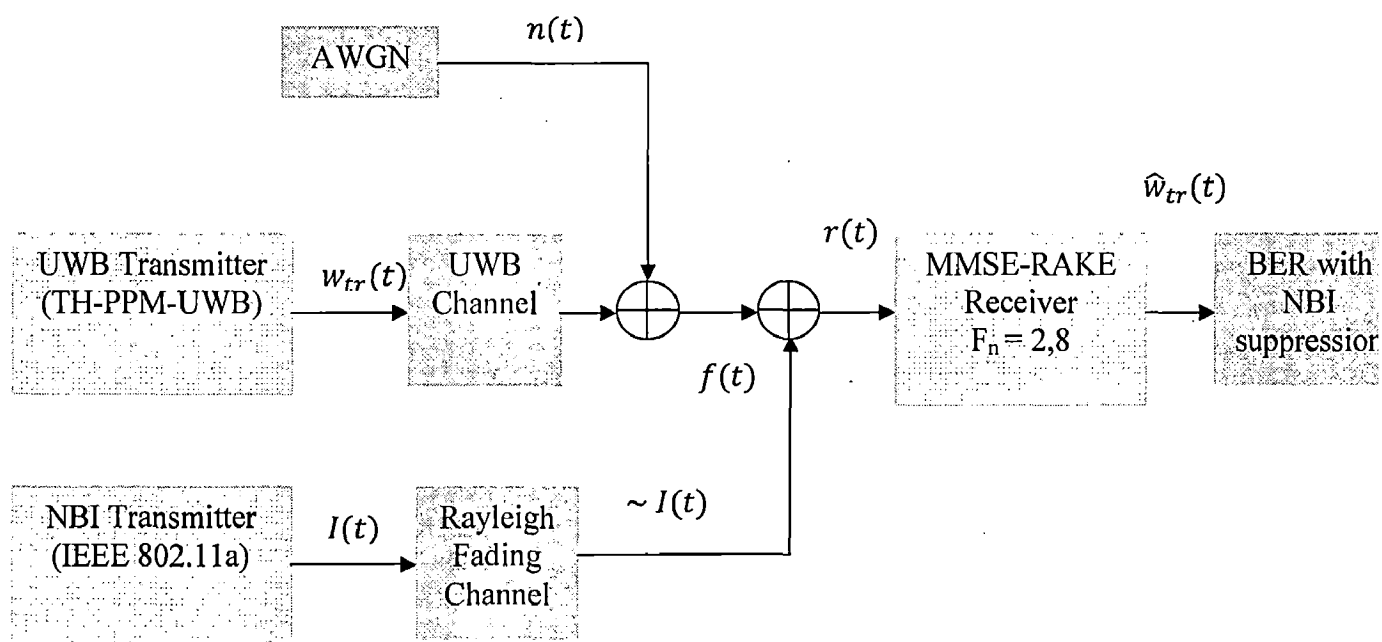


Figure 6.1 Simulation Block Diagram.

As shown in the simulation block diagram, the signal $w_{tr}(t)$ after passing through UWB communication channel and AWGN becomes $f(t)$. The NB signal $I(t)$ after passing through Rayleigh Fading channel becomes $\sim I(t)$. Signal $r(t)$ is the result of the addition between $f(t)$ and $\sim I(t)$. The NBI signal is being detected from $r(t)$ and suppressed. Signal $\hat{w}_{tr}(t)$ is the UWB signal recovered after NBI suppression. The symbol F_n denotes the number of fingers of



the rake receiver. The block BER With NBI suppression gives the results after the NBI is suppressed from the UWB system. These simulation results are available in section 6.3 based on MMSE-RAKE receiver analysis in Chapter 5.

6.2 Simulation Parameters

In Table 6.1 shows the parameter value of TH-PPM-UWB system, Table 6.2 shows the parameter value of NBI (IEEE 802.11a OFDM WLAN) and Table 6.3 shows the parameter value of IEEE 802.15.3a proposed CM1 Channel model (LOS 0-4 m), that is used in simulation.

TABLE 6.1

Value of the Principal Parameters for the TH-PPM-UWB System

Parameter	Symbol	Typical Value
Fudge factor	τ	0.2 ns
Impulse Width	T_P	0.5 ns
Frame Width	T_f	20 ns
Modulation Index	δ	0.15 ns
Chip Width	T_C	1 ns
Number of Hops	N_h	5, 10
Repetition Code Length	N_s	2
Number of bits	$d_{\lfloor j/N_s \rfloor}$	1000

TABLE 6.2

Value of the Principal Parameters for the NBI (OFDM System)

Parameter	Symbol	Typical Value
Total Number of Sub Carrier	N_{ST}	52
FFT Size	nFFT	64
Length of Cyclic Prefix	CP	16
Number of Transmitted Bits	nBit	1300

TABLE 6.3**Value of the Principal Parameters for CM1 UWB Channel (LOS 0-4 m)**

Parameter	Symbol	Typical Value
Cluster Arrival Rate	$\Lambda(1/ns)$	0.0223
Ray Arrival Rate	$\lambda(1/ns)$	2.5
Cluster Decay Factor	$\Gamma(ns)$	7.1
Ray Decay Factor	$\gamma(ns)$	4.3
Standard Deviation of Cluster Fading	$\sigma_1(dB)$	3.3941
Standard Deviation of Ray Fading	$\sigma_2(dB)$	3.3941
Standard Deviation of Lognormal Shadowing	$\sigma_x(dB)$	3

6.3 Simulation Results

In this section, present BER performance results based on analysis in section chapter 5, And simulated the decision variables indicated in equations (5.32) and (5.37). The parameters used for the simulation and their typical values are listed in Table 6.1 to Table 6.3. In our simulation, for calculation of the BER for TH-PPM-UWB systems, considered second-order Gaussian monocycle. And considered CM1 (LOS 0-4 m) UWB channel. However, simulation can be run for arbitrary pulse shapes with different values of N_s , and for other UWB channel such as CM2 (LOS 4-10 m), CM3 (NLOS 0-4 m) and CM4 (Extremely NLOS, Multipath channel).

The BER performance comparison of All RAKE, Selective RAKE and Partial RAKE receiver with MMSE combining for various Time Hopes and for different SIR are shows in upcoming sections.

6.3.1 BER for Different Number of MMSE-RAKE Finger

Fig. 6.2 shows BER performance of the for different number of MMSE-RAKE finger. Partial RAKE, combines the first arriving L_p paths without operating any selecting among all available multi-path components. As we can see, as number of RAKE finger increase in particular RAKE receiver, BER performance also improve. Like, performance of Partial MMSE-RAKE receiver for number of RAKE finger $N_h = 8$ ($L=8$) is better than number of RAKE finger $N_h = 2$ ($L=2$). As we can see, BER improvement with increasing SNR is better in Partial MMSE-RAKE receiver with number of RAKE finger $N_h = 8$ compare to Partial MMSE-RAKE receiver with number of RAKE finger $N_h = 2$. And All RAKE receiver, combined of all arriving multipath component, but this receiver increase complexity of receiver drastically compare to Partial MMSE-RAKE receiver. So as usual All MMSE-RAKE receiver outperform Partial MMSE-RAKE receiver since it achieves higher SNR at the output of the combiner.

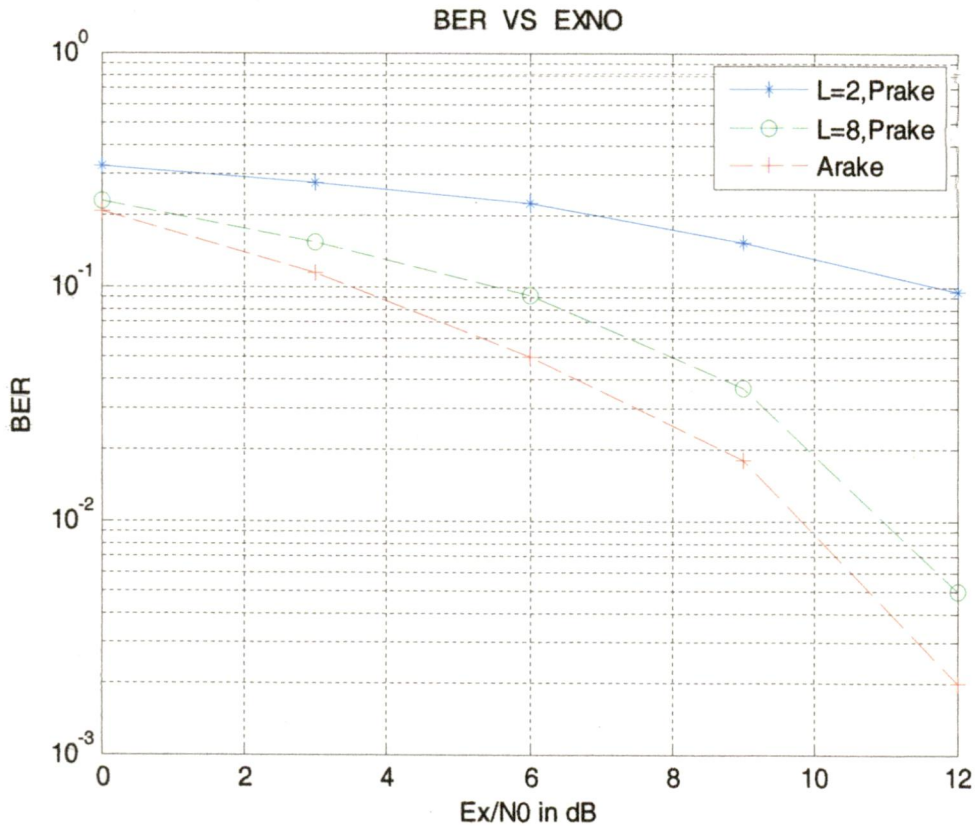


Figure 6.2 BER Performance for Partial MMSE-RAKE Receiver

Another strategy is called Selective RAKE, consists of selecting the L_B best components among the L_{TOT} available at the receiver input. From Fig. 6.3 can see, Selective MMSE-RAKE receiver

BER performance is improve with number of RAKE finger increase (S=2 to S=8). And again All RAKE receiver, combined of all arriving multipath component, So as expected All MMSE-RAKE receiver perform better than Selective MMSE-RAKE receiver.

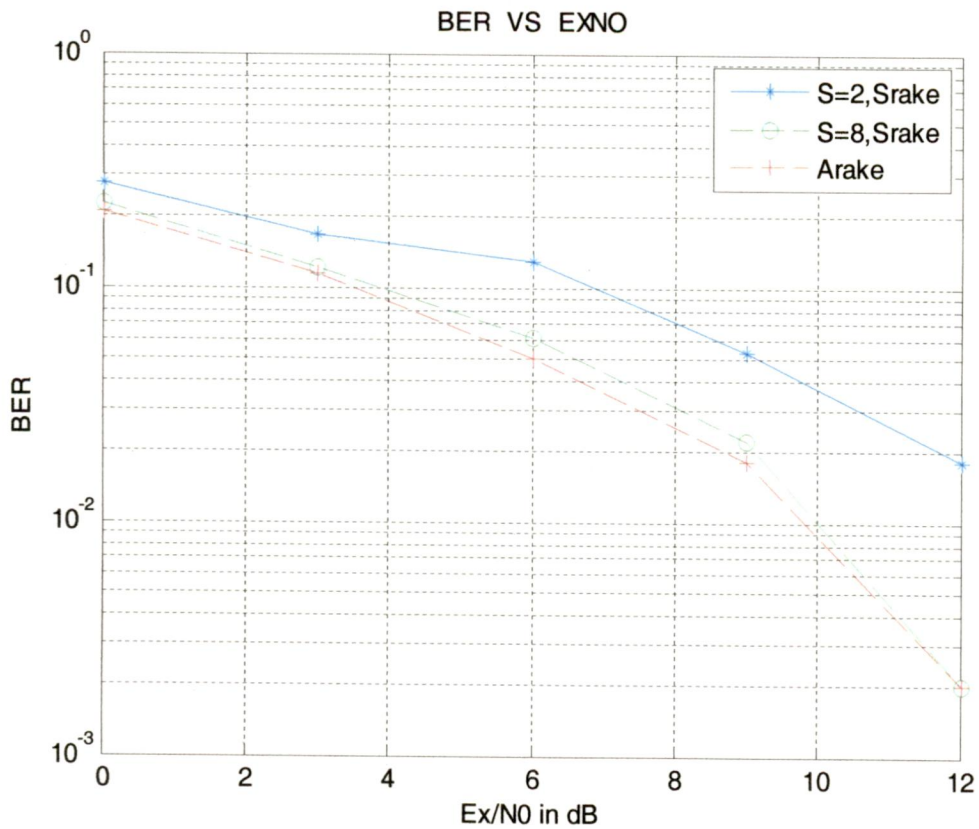


Figure 6.3 BER Performance for Selective MMSE-RAKE Receiver

Also from figure 6.4, can analysis the BER performance of P-RAKE, S-RAKE and A-RAKE receiver. The first strategy, called All RAKE receiver, combined of all arriving multipath component, but this receiver increase complexity of receiver drastically. Another strategy is called Selective RAKE, consists of selecting the L_B best components among the L_{TOT} available at the receiver input. The number of branches of the RAKE is reduced, but the receiver still must keep track of all the multi-path components to perform the selection. A third and simpler solution, called Partial RAKE, combines the first arriving L_P paths without operating any selecting among all available multi-path components. As expected, All RAKE outperform Selective RAKE and Partial RAKE. And Selective RAKE outperform Partial RAKE. The gap in performance, however, decreases when the best paths are located at the beginning of the channel impulse response as it happens, in general, when considering LOS scenarios.

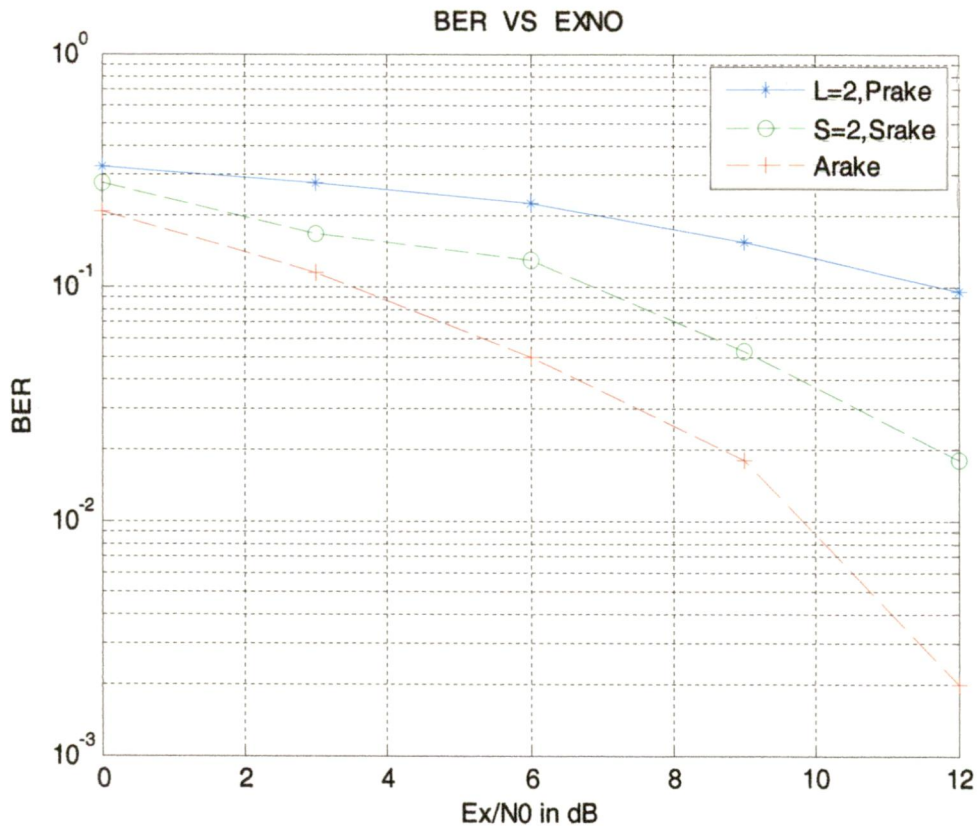


Figure 6.4 BER performance for different MMSE-RAKE receiver

6.3.2 BER for MMSE-RAKE Receiver for Different TH-Sequence

Fig. 6.5 shows BER performance of the for All MMSE-RAKE receiver for different number of Time Hopping sequence. As fig. shows with increasing Time hopping sequence number, BER performance of All RAKE receiver not improve much. Cause All RAKE receiver, combined of all arriving multipath component, So it already given best performance in compare to other RAKE receiver. So even for increasing Time hopping sequence number BER performance for NBI suppression not improve much. But for high SNR at input of receiver, All-RAKE receiver perform better for more Time hopping sequence. But in case of MAI (Multiple Access Interference), increasing Time hopping sequence number effect more. It improve the BER performance of All-RAKE receiver drastically [35].

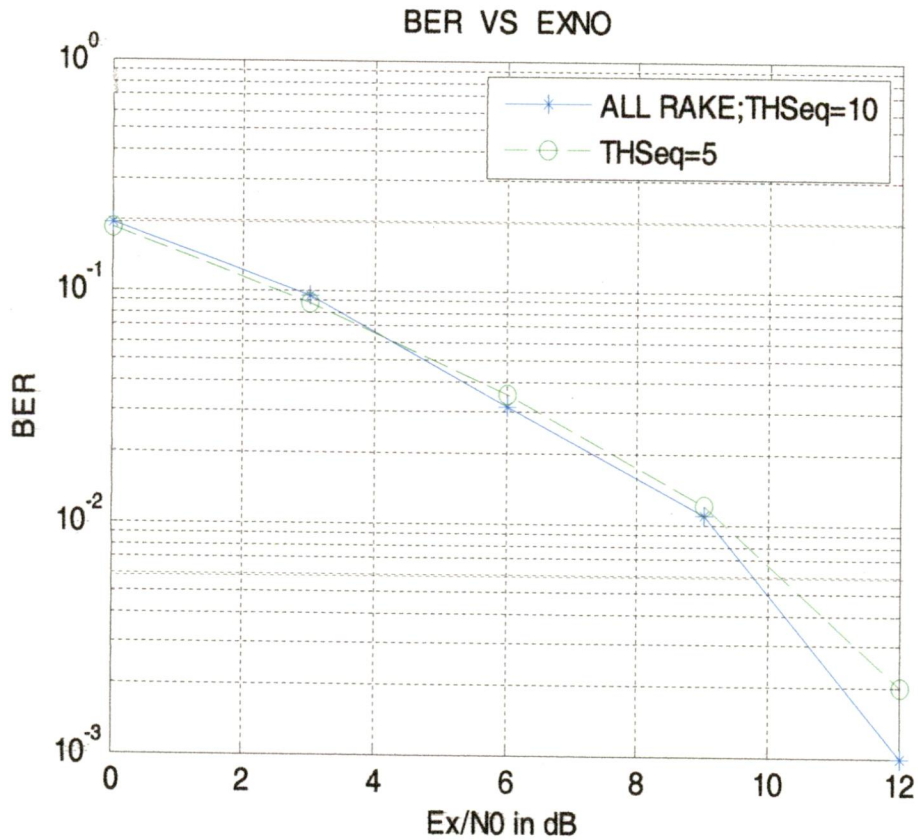


Figure 6.5 BER performance for All MMSE-RAKE receiver for different Time hopping sequence ($N_h=5$ and $N_h=10$)

Figure 6.6 shows BER performance of the for Selective MMSE-RAKE receiver for different number of Time Hopping sequence. As figure shows with increasing Time hopping sequence number, BER performance of Selective RAKE receiver is improve with SNR. Again for high SNR at input of receiver, Selective-RAKE receiver perform better for more Time hopping sequence.

Fig 6.7 shows BER performance of the for Partial MMSE-RAKE receiver for different number of Time Hopping sequence. As both figure show for high SNR at input of receiver, BER improvement in Selective Rake receiver is better than Partial Rake receiver. Number of Rake finger uses for both simulation is 8 ($F_n=8$). And different TH sequence is 5 and 10 ($N_h= 5$ and 10).

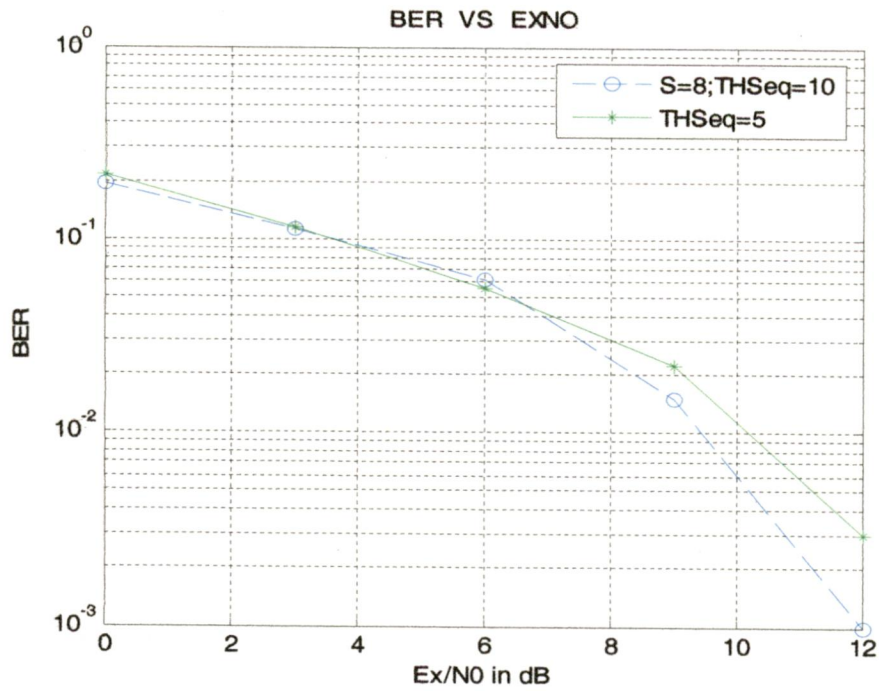


Figure 6.6 BER performance for Selective MMSE-RAKE receiver for Different Time Hopping Sequence ($N_h=5$ and $N_h=10$)

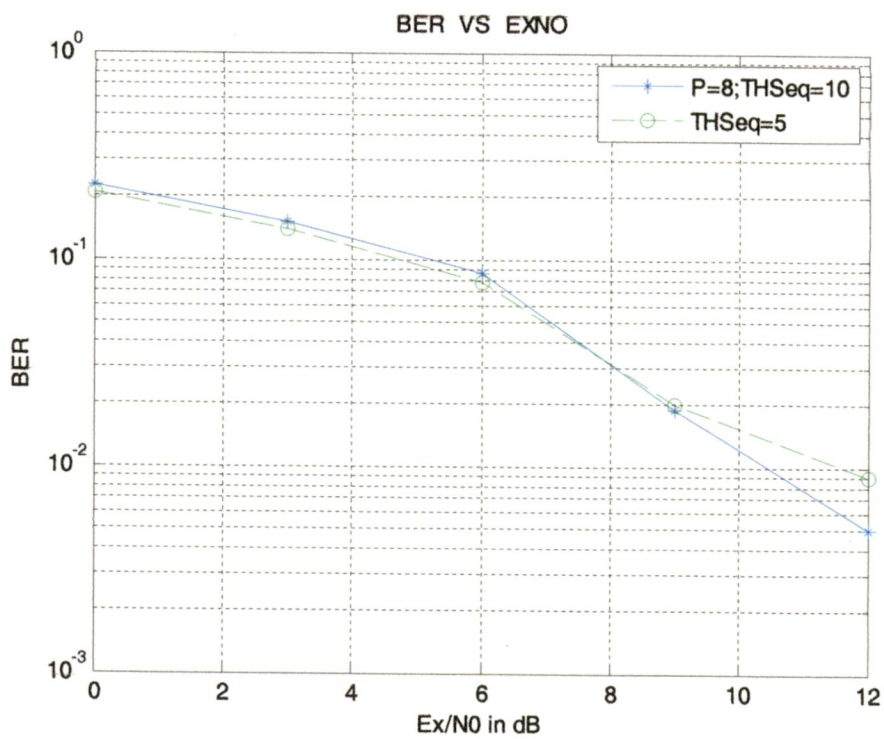


Figure 6.7 BER performance for Partial MMSE-RAKE receiver for Different Time Hopping Sequence ($N_h=5$ and $N_h=10$)

6.3.3 BER for MMSE-RAKE Receiver for Different SIR

Fig. 6.8 shows BER performance of the for All MMSE-RAKE receiver for different signal to interference ratio (SIR) that is given by equation (5.49). As figure show, even with increasing SIR at input of receiver BER performance of All Rake receiver is not much changes, even with increasing SIR for high SNR at input of receiver, BER performance of All RAKE receiver is almost similar.

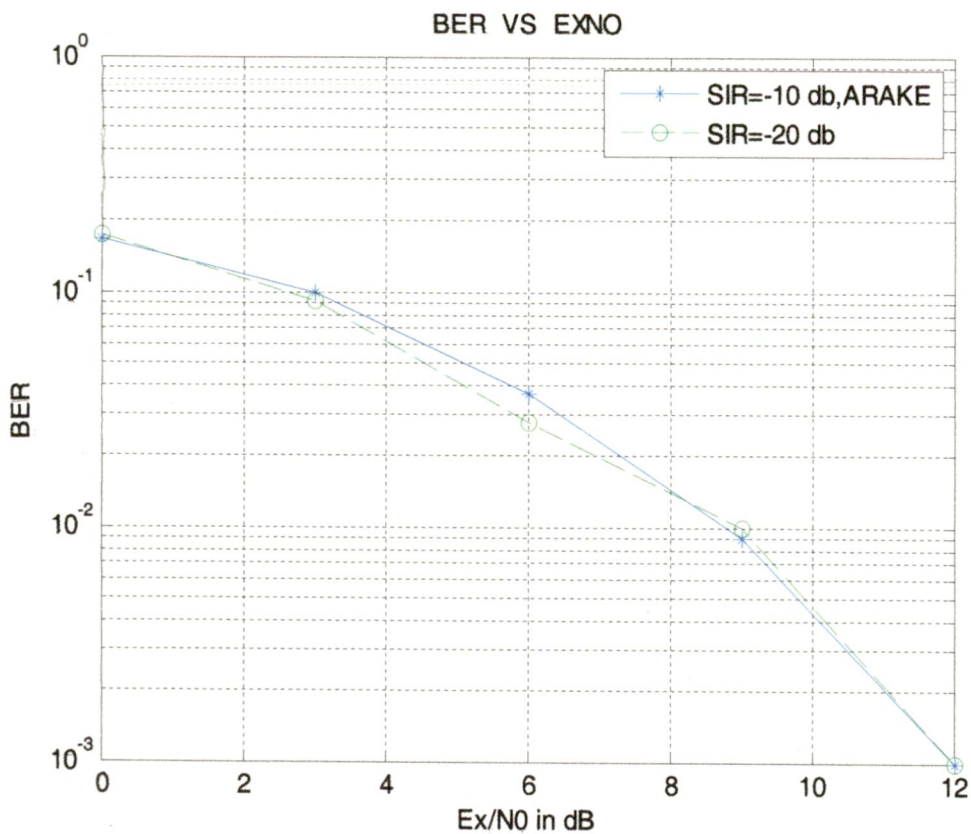


Figure 6.8 BER performance for All MMSE-RAKE receiver for different SIR (SIR = -10dB and -20dB)

Fig. 6.9 shows BER performance of the for Selective MMSE-RAKE receiver for different SIR. As fig. shows for high SNR at input of receiver BER performance of S-RAKE is improve a lot with increasing SIR. Fig 6.9 and Fig 6.10 also shows that, for high SNR, the BER performance of S-RAKE receiver even when SIR is -20 dB is better than P-RAKE receiver (when SIR= -10 dB for P-RAKE receiver).

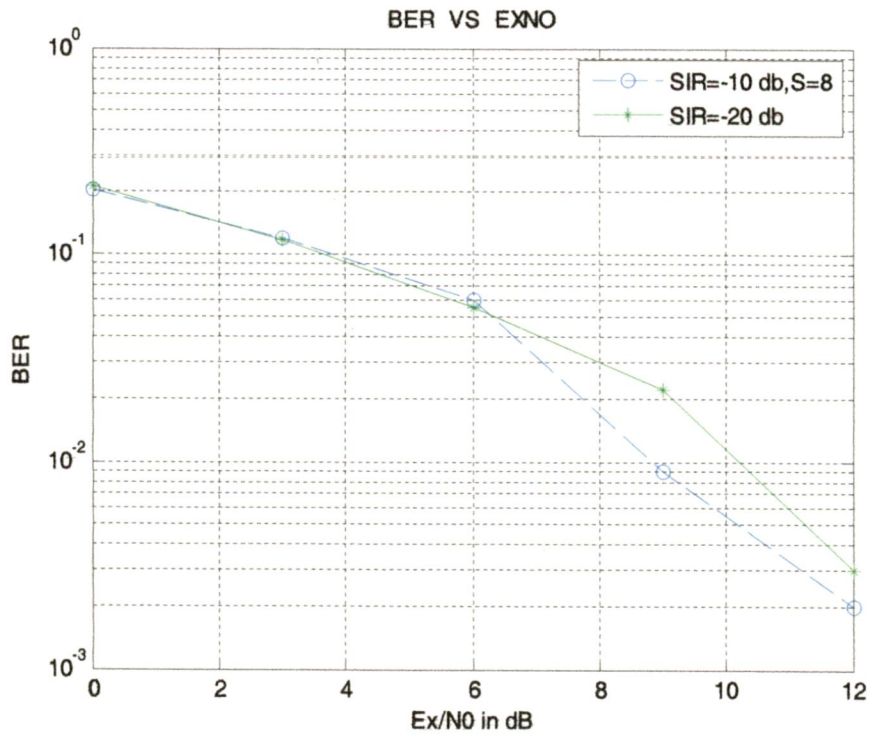


Figure 6.9 BER performance for Selective MMSE-RAKE Receiver for Different SIR (SIR = -10dB and -20dB)

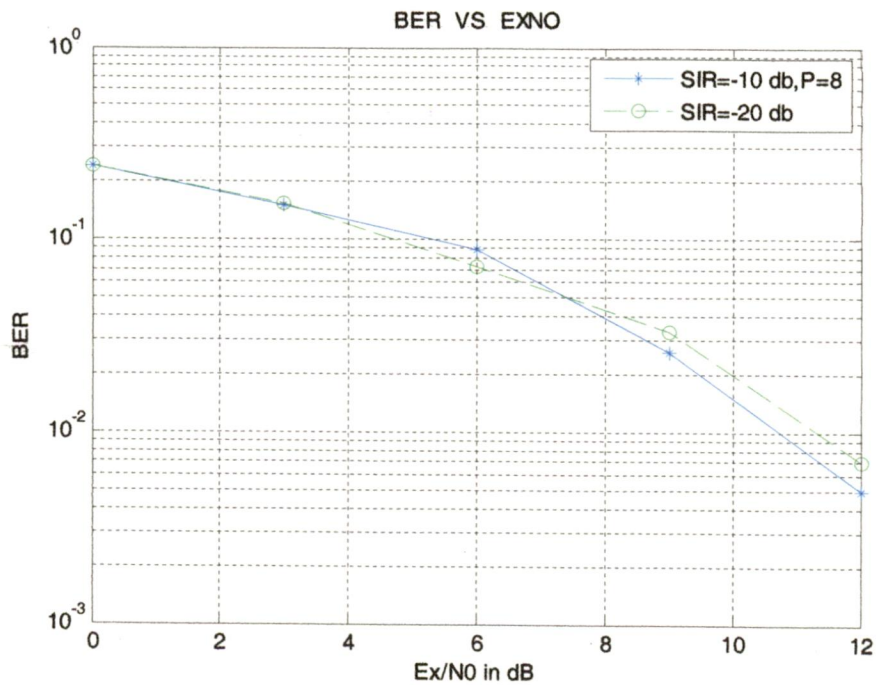


Figure 6.10 BER performance for Partial MMSE-RAKE Receiver for Different SIR (SIR = -10dB and -20dB)

CONCLUSION AND FUTURE WORK

The TH-PPM-UWB system was analyzed in a realistic UWB frequency selective channel and in the presence of NBI for various time hopping sequence lengths and for different SIR. From previous work it demonstrated that TH reduces the impact of multiuser interference but does not combat NBI. To suppress NBI, a MMSE-Rake multipath diversity receiver was described and the effect of OFDM signal as NBI signals was investigated.

A major advantage of the MMSE scheme, relative to other interference suppression schemes, is that explicit knowledge of interference parameters is not required. The received signal can be sampled at the pulse repetition frequency after passing through the correlation receiver and the samples are linearly combined using the MMSE criterion, so that the weights are chosen to suppress the NBI.

In chapter 5, The conditional bit error rate performance, the SNIR at the output of the selective rake receiver combiner as well the system data rate performance were analytically evaluated as a function of the number of the selected paths as well as the NBI characteristics. In chapter 6, Results show that for a realistic UWB indoor channel, the MMSE-Rake receiver is able to combat NBI with an SIR as high as -20 dB. In addition, simulation results shows BER performance comparison of All MMSE-RAKE, Selective MMSE-RAKE and Partial MMSE-RAKE receiver for NBI suppression for various TH and different SIR. In particular, even the partial MMSE-RAKE receiver can achieve a high level of NBI suppression, crucial for any UWB receiver, while requiring only a small modification of the traditional Rake receiver.

The UWB system in this report is assumed to be perfect synchronization and accurate signal acquisition with the second order Gaussian mapping waveform. Future works can be extended to non-ideal synchronization and signal acquisition with higher order of Gaussian mapping waveforms. And also Future works can be extended to adaptive minimum mean square error (MMSE) Rake receiver for UWB-IR system in multipath channels to suppress Narrowband Interference (NBI).

REFERENCES

- 1 Maria-Gabriella Di Benedetto, Guerino Giancola, *Understanding Ultra WideBand Radio Fundamentals*, New Jersey, United State, Prentice Hall, 2004.
- 2 Hui Yu, Enrique Aguado, Gary Brodin, John Cooper, David Walsh and Hal Strangeways, "UWB Positioning System Design: Selection of Modulation and Multiple Access Schemes" *Journal of Navigation ISSN 0363-4633*, vol. 61, no. 1, 2008, pp. 45-62.
- 3 Defense Advanced Research Projects Agency, Office of the Secretary of Defense, "Assessment of Ultra-Wideband (UWB) Technology," Report R-6280, prepared by OSD/DARPA UWB Radar Review Panel, July 1990.
- 4 Huseyin Arslan, Zhi Ning Chen, Maria-Gabriella Di Benedetto, *Ultra Wideband Wireless Communication*, New Jersey, United State, John Wiley & Sons Ltd, 2006.
- 5 J.D. Choi and W.E. Stark, "Performance analysis of ultra-wideband spreading spectrum Communications in narrowband interference," *IEEE MILCOM*, vol. 21, October 2002, pp. 1075-1080.
- 6 Li Zhao, Alexander M. Haimovich and Haim Grebel, "Performance of UWB communications in the presence of interference," *IEEE Journal on Selected Areas in Communication*, vol. 20, issue 9, December 2002, pp. 1684-1691.
- 7 Matti Hamalainen, Raffaello Tesi, and Jari Iinatti, "UWB Co-Existence with IEEE 802.11a and UTMS in Modified Saleh-Valenzuela Channel," available at http://www.ee.oulu.fi/~matti/i/WUWBS2004_ID034.pdf.
- 8 J. H. Reed, Ed., *An Introduction to Ultra Wideband Communication Systems*, Englewood Cliffs, NJ: Prentice-Hall, 2005.
- 9 I. Bergel, E. Fishler, and H. Messer, "Narrow-band interference suppression in time-hopping impulse-radio systems," in *Proc. IEEE UWBST*, 2002, PP. 303-306.
- 10 Andrea Giorgetti, Marco Chiani, and Moe Z. Win, "The Effect of Narrowband Interference on Wideband Wireless Communication Systems," *IEEE Trans. on Communication*, vol. 53, no.12, December 2005, pp. 2139-2149.
- 11 L. Piazza and F. Ameli, "Performance analysis for impulse radio and direct-sequence impulse radio in narrowband interference," *IEEE Trans. on Communication*, vol. 53, no. 9, Sep. 2005, pp. 1571-1580.

- 12 J. R. Foerster, "The performance of a direct-sequence spread ultra wideband system in the presence of multipath, narrowband interference, and multiuser interference," in *Proc. IEEE UWBST*, 2002, pp. 87–91.
- 13 L. Yang and G. B. Giannakis, "Unification of ultra-wideband multiple access schemes and comparison in the presence of interference," in *Proc. IEEE Asilomar Conf.*, 2003, vol. 2, pp. 1239–1243.
- 14 L. Yang and G. B. Giannakis, "A general model and SINR analysis of low duty-cycle UWB access through multipath with narrowband interference and rake reception," *IEEE Trans. on Wireless Communication*, vol. 4, no. 4, Jul. 2005, pp. 1818–1833.
- 15 M. Hamalainen, V. Hovinen, R. Tesi, J. Iinatti, and M. Latva-aho, "On the UWB system coexistence with GSM900, UMTS/WCDMA, and GPS," *IEEE Journal on Selected Areas in Communication*, vol. 20, no. 9, Dec. 2002, pp. 1712–1721.
- 16 M. S. Iacobucci, M. G. Di Benedetto, and L. De Nardis, "Radio frequency interference issues in impulse radio multiple access communication systems," in *Proc. UWBST*, 2002, pp. 293–296.
- 17 A. Taha and K. M. Chugg, "A theoretical study on the effects of interference UWB multiple access impulse radio," in *Proc. IEEE Asilomar Conf.*, vol. 1, 2002, pp. 728–732.
- 18 W. Tao, W. Yong, and C. Kangsheng, "Analyzing the interference power of narrowband jamming signal on UWB system," in *Proc. IEEE PIMRC*, vol. 1, 2003, pp. 612–615.
- 19 Z. Luo, H. Gao, Y. Liu, and J. Gao, "A new UWB pulse design method for narrowband interference suppression," in *Proc. GLOBECOM*, Nov. 29, vol. 6, 2004, pp. 3488–3492.
- 20 Li Qinghua and L. A. Rusch, "Multiuser receivers for DS-CDMA UWB," in *Proc. IEEE Conf. on Ultra Wideband Systems and Technologies*, May 2002, pp. 163-168.
- 21 Weihua Zhuang, Xuemin (Sherman) Shen and Qi Bi, *Ultra-wideband Wireless Communications*, John Wiley & Sons Ltd, 2003.
- 22 William Stallings, *Wireless Communications and Networks*, Prentice Hall, November 2004.
- 23 Theodore S. Rappaport, *Wireless Communications: Principles and Practice*, Prentice Hall, 2007.
- 24 L. Yang and G. B. Giannakis, "Ultra-Wideband Communications," *IEEE Signal Processing Magazine*, Nov 2004, pp. 26-54.

- 25 Price, R., and P.E. Green Jr., "A communication technique for multi-path channels," *Proc. IRE*, vol. 46, March 1958, pp. 555-570.
- 26 Win, M.Z., and R.A. Scholtz, "On the Robustness of Ultra-Wide Bandwidth Signals in Dense Multipath Environments," *IEEE Communication Letters*, vol. 2, issue 2, February 1998, pp. 51-53.
- 27 Nejib Boubaker and Khaled Ben Letaief, "A Low Complexity MMSE-RAKE Receiver in a Realistic UWB Channel and in the Presence of NBI" *IEEE Conf. on Wireless Communications*, Mar. 2003, pp. 233-237.
- 28 Cassioli, D., M.Z. Win, F. Vatalaro, and A.F. Molisch, "Performance of Low Complexity Rake Reception in a Realistic UWB Channel," *IEEE International Conf. on Communications*, vol. 2, April 2002, pp. 763-767.
- 29 M. Ghavami, L. B. Michael, R. Kohno, *Ultra Wideband Signals and Systems in Communication Engineering*, West Sussex, England, John Wiley & Sons Ltd, May 2004.
- 30 Marc Engels, *Wireless OFDM systems: how to make them work?*, Boston, USA, Kluwer Academic Publishers, 2002.
- 31 Qinghua Li and Leslie A. Rusch, "Multiuser detection for DS-CDMA UWB in the home environment," *IEEE Journal on Selected Areas in Communications*, vol. 20, issue 9, December 2002, pp. 1701-11.
- 32 D. Cassioli, M. Z. Win, F. Vatalaro, and A. F. Molisch, "Performance of low-complexity rake reception in a realistic UWB channel," in *Proc. IEEE International Conf. on Communications*, vol. 2, Apr. 2002, pp. 763-767.
- 33 K. Wang and Y. Bar-Ness, "The prediction MMSE receiver for joint multiple-access and narrow-band interference suppression in DS/CDMA channels," in *Proc. IEEE International Conf. on Communications*, vol. 2, June 2000, pp. 909-913.
- 34 J. Foerster, "UWB channel modeling sub-committee report final," *IEEE P802.15 Working Group for Wireless Personal Area Networks (WPANs)*, Feb. 2003.
- 35 Nejib Boubaker, Khaled Ben Letaief, "MMSE Multipath Diversity Combining for Multi-Access TH-UWB in the Presence of NBI," *IEEE Trans. on Wireless Communication*, vol. 5, no. 4, April 2006, pp. 712-719.